

2002

Approaches to measuring the frequency of achondroplasia and hypochondroplasia causing FGFR-3 mutations in human sperm

Andrew Timothy Daters

Louisiana State University and Agricultural and Mechanical College

Follow this and additional works at: https://digitalcommons.lsu.edu/gradschool_theses



Part of the [Veterinary Medicine Commons](#)

Recommended Citation

Daters, Andrew Timothy, "Approaches to measuring the frequency of achondroplasia and hypochondroplasia causing FGFR-3 mutations in human sperm" (2002). *LSU Master's Theses*. 130.
https://digitalcommons.lsu.edu/gradschool_theses/130

This Thesis is brought to you for free and open access by the Graduate School at LSU Digital Commons. It has been accepted for inclusion in LSU Master's Theses by an authorized graduate school editor of LSU Digital Commons. For more information, please contact gradetd@lsu.edu.

APPROACHES TO MEASURING THE FREQUENCY OF
ACHONDROPLASIA AND HYPOCHONDROPLASIA CAUSING FGFR-3
MUTATIONS IN HUMAN SPERM

A Thesis

Submitted to the Graduate Faculty of the
Louisiana State University and
Agricultural and Mechanical College
in partial fulfillment of the
requirements for the degree of
Master of Science

The Interdepartmental Program
In Veterinary Medical Sciences

through

The Department of Comparative Biomedical Sciences

by
Andrew T. Daters
B.S., Washington and Lee University, 1997
August 2002

ACKNOWLEDGEMENTS

I would like to first thank my parents who gave me the utmost encouragement and support through all of my academic endeavors. I would also like to thank my patient wife, Callie, without whom the real funding of this project would not be possible. Finally, I would like to thank Dr. Vince Wilson who was the only one out there willing to take a down on his luck student under his wings. And to the one who sat with me from page 1 until the end and gave up many afternoon walks, I would like to thank my dog, Goose.

TABLE OF CONTENTS

ACKNOWLEDGEMENTS	ii
LIST OF TABLES	v
LIST OF FIGURES.....	vi
ABSTRACT	viii
CHAPTER 1. INTRODUCTION	1
CHAPTER 2. FIBROBLAST GROWTH FACTORS	3
CHAPTER 3. FIBROBLAST GROWTH FACTOR RECEPTORS	5
CHAPTER 4. FIBROBLAST GROWTH FACTOR RECEPTOR 3	12
CHAPTER 5. SKELETAL DYSPLASIAS	15
5.1 ACHONDROPLASIA	15
5.2 HYPOCHONDROPLASIA	18
CHAPTER 6. MUTATIONS AND DISEASE.....	22
CHAPTER 7. APPROACH	33
7.1 APPROACH AT THE HYPOCHONDROPLASIA SITE.....	34
7.2 APPROACH AT THE ACHONDROPLASIA SITE.....	35
CHAPTER 8. MATERIALS AND METHODS	40
8.1 NEEDLE-IN-A-HAYSTACK ASSAY	40
8.2 HYPOCHONDROPLASIA SITE.....	41
8.2.1. MUTANT PCR AND RESTRICTION ENDONUCLEASE (PCR/RE) SELECTION OF THE HYPOCHONDROPLASIA SITE	41
8.2.2 LCR AND PAGE OF THE HYPOCHONDROPLASIA SITE	42
8.3 ACHONDROPLASIA SITE.....	42
8.3.1 MUTANT PCR AND RESTRICTION ENDONUCLEASE (PCR/RE) SELECTION OF THE ACHONDROPLASIA SITE	42
8.3.2 LCR AND PAGE OF THE ACHONDROPLASIA SITE	43
CHAPTER 9. RESULTS.....	45
9.1 RESULTS OF THE PCR/RE/LCR OF THE HYPOCHONDROPLASIA SITE.....	45
9.2 INCORPORATION OF A <i>Msp</i> I RESTRICTION SITE.....	46
9.3 DESIGN OF THE SECOND VERSION OF THE LCR ASSAY AT SITE 1620	53
9.4 LCR RESULTS FOR SITE 1620.....	53
9.5 DESIGN OF THE THIRD VERSION OF THE LCR ASSAY AT SITE 1620.....	67
9.6 ALLELE SPECIFIC PCR RESULTS FOR SITE 1138.....	72

CHAPTER 10. DISCUSSION	85
CHAPTER 11. CONCLUSIONS.....	90
REFERENCES.....	92
VITA	101

LIST OF TABLES

Table 1. FGFR-3 Missense mutations diseases.....	29
Table 2. Version 1 primer sequences and annealing temperatures for the PCR/RE selection of the C1620A/G base change	35
Table 3. Primer sets, annealing temperatures, and PCR product length of the Version 1 PCR protocol for the Hypochondroplasia site.....	35
Table 4. LCR Version 1 primers and size in base pairs for the Hypochondroplasia site	36
Table 5. Sizes of LCR product, from both sense and antisense strands.....	36
Table 6. Version 1 primer sequences and annealing temperatures for the PCR/RE selection of the G1138A/C base change	38
Table 7. Primer sets, annealing temperatures, and PCR product length of the achondroplasia site.....	38
Table 8. LCR assay for the achondroplasia site 1138	38
Table 9. Sizes of LCR product, from both sense and antisense strands.....	39
Table 10. Version 2 primer sequences and annealing temperatures for the PCR/RE selection of the C1620A/G base change	45
Table 11. Version 3 primer sequences and annealing temperatures	51
Table 12. LCR Version 2 primers and size in base pairs	56
Table 13. Sizes of LCR product, from both sense and antisense strands.....	56
Table 14. Amount of mutant DNA combined with 6 µg of wild-type DNA	67
Table 15. LCR Version 3 primers and size in base pairs	69
Table 16. Sizes of LCR product, from both sense and antisense strands.....	69
Table 17. Primer sequences and sizes for the allele specific PCR technique	73
Table 18. Primer sequences and sizes for the allele specific PCR technique	83

LIST OF FIGURES

Figure 1. Schematic representation of the FGFR-3 protein	6
Figure 2. Schematic representation of a dimerized FGFR-3 complex.....	9
Figure 3. Schematic representation of the FGFR-3 protein	30
Figure 4. Graphic representation of ACH and HCH mutations	31
Figure 5. LCR primer design for the detection of mutated sequences.....	37
Figure 6. Agarose gel of the PCR products and restriction products.....	47
Figure 7. Agarose gel of the PCR products of primer set S-ZR	48
Figure 8. Agarose gel of the PCR products of primer set T-YR.....	49
Figure 9. Autoradiograph a first version LCR	50
Figure 10. Schematic representation of the incorporation of the restriction endonuclease recognition sequence	52
Figure 11. Agarose gel of successful nested PCR/RE sequences	54
Figure 12. Agarose gel of successful PCR with primer set S-MspIR	55
Figure 13. LCR primer design for the detection of mutated sequences	57
Figure 14. Autoradiograph of a second version LCR testing the Wt and Mt primers ...	59
Figure 15. Autoradiograph of an LCR test.....	61
Figure 16. Autoradiograph of an LCR run at 64°C.....	62
Figure 17. Autoradiograph of an LCR testing progressively decreasing concentrations of oligonucleotide standard T	64
Figure 18. Autoradiograph of an LCR run at 62°C.....	66
Figure 19. Autoradiograph of the 2 nd version LCR with the selection process	68
Figure 20. Autoradiograph of an LCR run at 65°C.....	70
Figure 21. Autoradiograph of an LCR of the selection process.....	74

Figure 22. Autoradiograph of LCR selection process using a mutant primer mix	75
Figure 23. Schematic representation of the allele specific PCR at site 1138.....	76
Figure 24. Agarose gel of the test run with the allele specific wild-type and mutant primers at 60°C	78
Figure 25. Agarose gel of the test run with the allele specific wild-type and mutant primers at 65°C	79
Figure 26. Agarose gel of the test run with the allele specific wild-type and mutant primers at 58°C	80
Figure 27. Agarose gel of the test run with the allele specific wild-type and mutant primers at 59°C	81
Figure 28. Agarose gel of the test run with the allele specific wild-type and mutant primers at 59°C using ½ the amount of template DNA	82
Figure 29. Agarose gel of the test run with second set of the allele specific wild-type and mutant primers	84

ABSTRACT

Achondroplasia and hypochondroplasia are two forms of skeletal dysplasias caused predominantly by single base mutations in the fibroblast growth factor receptor 3 gene (FGFR-3). The mutation for achondroplasia is a G1138A/C substitution and the mutation for hypochondroplasia (occurring about 50% of the time) is a C1620A/G substitution. Recent genetic studies have shown that spontaneous mutations for achondroplasia and hypochondroplasia occur exclusively on the paternally derived chromosome, suggesting that these mutations occur preferentially during spermatogenesis. For unknown reasons, the mutation rates at these FGFR-3 nucleotides appear to occur at a much higher frequency than nucleotide specific mutation rates observed in other human genetic diseases.

The purpose of this study was to develop an assay that could detect the frequencies of achondroplasia and hypochondroplasia causing mutations in human sperm. A Needle-in-a-Haystack PCR/RE/LCR selection technique has been developed that measures single base changes, commonly single base substitution mutations, at sensitivities of one mutant allele in one cell in up to 10^7 wild-type cells. This technique was modified and designed for the achondroplasia and hypochondroplasia base sites 1138 and 1620 of the FGFR-3 gene. With the development of this technique, future studies could focus on determining the frequencies of the mutations in the sperm of fathers of affected children and the frequencies of the mutations in the sperm of the normal population. These studies will help elucidate the paternal age effect, have important implications in genetic counseling and provide a novel method by which to study genetic disease in humans.

CHAPTER 1. INTRODUCTION

The fibroblast growth factors are a complex family of mammalian signaling molecules. Their interaction with their corresponding family of fibroblast growth factor receptors constitutes a very dramatic cell signaling pathway responsible for many different molecular processes. Many human disease processes have been linked with faulty growth factors and/or growth factor receptors. Two such diseases, achondroplasia and hypochondroplasia, are caused by single base mutations in the fibroblast growth factor receptor 3 (FGFR-3) gene.

These mutations to the FGFR-3 gene result in the constitutive activation of the receptor and its subsequent cell signaling pathway. Through a complex series of molecular events, the insult to FGFR-3 alters the finely tuned process of long bone growth and development leading to varying forms of short-limb dwarfism.

The incidence of short-limb dwarfism in the population is between 1 in 15,000 and 1 in 40,000 live births. This high degree of incidence makes the FGFR-3 gene one of the most mutation prone genes in the human genome. In addition to the high rate of mutation, these mutations in an affected individual are derived from the paternal allele. A paternal age effect has also been shown for these mutations.

Because the achondroplasia and hypochondroplasia mutations are both derived from the paternal allele, and because there is an increased incidence with advanced paternal age, it is believed that germline mutations are responsible for the development of the disease in offspring. It is not known, however, whether these germline mutations occur early in the development of sperm stem cells, or later in the processes of spermatogenesis.

It is also unknown as to whether or not the mutation is found through the entire population of stem cells, or rather, in an isolated pocket of mutated stem cells.

For these reasons, it would be very beneficial to be able to determine the frequency of the achondroplasia and hypochondroplasia causing mutations in a population of human sperm. The ability to compare these frequencies in the sperm of males with affected offspring, to affected males, and to normal individuals would be very beneficial in determining the origin and effects of these germline mutations.

This project focused on creating an approach to measuring the frequency of achondroplasia and hypochondroplasia causing FGFR-3 mutations in human sperm. This would be accomplished by designing a highly sensitive assay that could detect one mutated genome in a background population of one million wild-type cells. In future endeavors, this assay could then be used to measure the frequency of the mutations in the sperm of fathers with affected offspring, affected individuals, and normal males.

CHAPTER 2. FIBROBLAST GROWTH FACTORS

The fibroblast growth factors are a family of structurally related proteins that are responsible for a wide array of control and signaling in many biological systems. To date, over twenty different types of fibroblast growth factors (FGFs) have been discovered, called FGF-1 to FGF-23. All of these proteins have been defined as FGFs because of two characteristics. The first is that they all contain a central core of 140 amino acids that are highly homologous throughout the classes of these FGF proteins. This core forms twelve antiparallel β -strands that together construct a cylindrical barrel that is enclosed by the variable region of the growth factors. The second characteristic is that they all have a high binding affinity for heparin and heparin-like glycosaminoglycans (HLGAGs) (Ago et al. 1991, Zhang et al. 1991). These are the defining features that place a polypeptide in the FGF family, not specificity of growth promoting activity. In fact, some FGFs do not stimulate fibroblasts at all. Therefore, these factors are given the name FGF family based on structure, not function (Baird and Klagsbrun 1991).

FGFs are produced in almost every cell of the body. The amount of the respective FGF depends on the time of development and what organ is being examined. For instance, FGF-3 is produced primarily during early embryonic development while FGF-9 was isolated from mature glial cell lines (Basilico and Moscatelli 1992, Miyamoto et al. 1993).

After the FGFs are produced, they are secreted from the cells into the extracellular matrix (ECM) by one of two mechanisms. Most FGFs use the classic endoplasmic reticulum-Golgi body pathway of secretion. FGFs-1, -2, and -9 use an as of yet undefined endoplasmic reticulum-Golgi body independent pathway. In the ECM, the factors bind the heparin molecules and serve as a spatially regulated reservoir outside of the cells. The

polypeptide can then either remain in the ECM to act on cells in close proximity, or it can be digested from the matrix and bind to a FGF binding protein and be carried away from its immediate environment to act on more remote cells (Folkman et al. 1988).

The functions of the FGFs are almost as variable as the number of different growth factors. FGFs have demonstrated the ability to be potent mitogens in vitro for cells of mesodermal, ectodermal, and neuroectodermal origin. In addition to the FGFs' proliferative nature in vitro, FGFs can also modify a target cell's motility, differentiation, extension of neuritis, and survival. These molecules have also been implicated in vivo in serving as major components of such processes as embryonic and fetal development, neovascularization, and response to healing. Regulation of growth by FGFs is aided by the nature of the protein in the ECM. When the FGFs are bound to heparin molecules that are confined to the ECM, only the cells in direct contact with the ECM can be targeted. This is very important in regulating the growth of developing limbs in the embryo as well as new vascularization and tissue proliferation throughout life. As a result of the importance of FGFs in new tissue formation, some FGFs have also been implicated to play a role in tumor growth and development (Powers et al. 2000).

The large number of different types of FGFs and the wide range of their functions demand a complex signaling system. The role of the FGF is carried out by its binding to the fibroblast growth factor receptor (FGFR).

CHAPTER 3. FIBROBLAST GROWTH FACTOR RECEPTORS

The important relationship between FGFs and fibroblast growth factor receptors (FGFRs) has been a major focus of study for the past decade. Moscatelli initiated the belief that fibroblast receptors existed in 1987. By using radiolabeled FGF-2, he found that the protein bound with high affinity to a protein on the surface of baby hamster kidney (BHK) cells. Studies then determined that these FGFs were binding to a high affinity site of a protein that was between 125 and 160 kDa (Blanquet et al. 1989).

The first breakthrough to as to the overall structure of the FGFR protein occurred in 1989. The proteins at the high affinity binding sites were isolated from chicken embryos and their amino acid sequence was determined. Using oligonucleotide probes based on this protein sequence, the receptor cDNA was cloned. (Lee et al. 1989) The first FGF receptor was found to be a single unit transmembrane protein made up of three parts. The first part is an extracellular region containing three extracellular immunoglobulin-like domains, which is the ligand-binding domain of the receptor. The immunoglobulin-like domains were named IgI, IgII, and IgIII. It was also discovered that there was an acidic region between IgI and IgII. The second region was a transmembrane domain. The third region was an intracellular unit that consisted of a tyrosine kinase domain (Figure 1.).

The discovery of the intracellular tyrosine kinase domain reinforced earlier studies by Coughlin et al. (1988) as to the mechanism of the FGF receptor. In these studies, they showed that FGF-1 and FGF-2 stimulated tyrosine phosphorylation in certain strains of fibroblast cells by using phosphotyrosine antibodies and Western blot staining. These techniques were used to define the first two FGF receptors named FGFR-1 and FGFR-2.

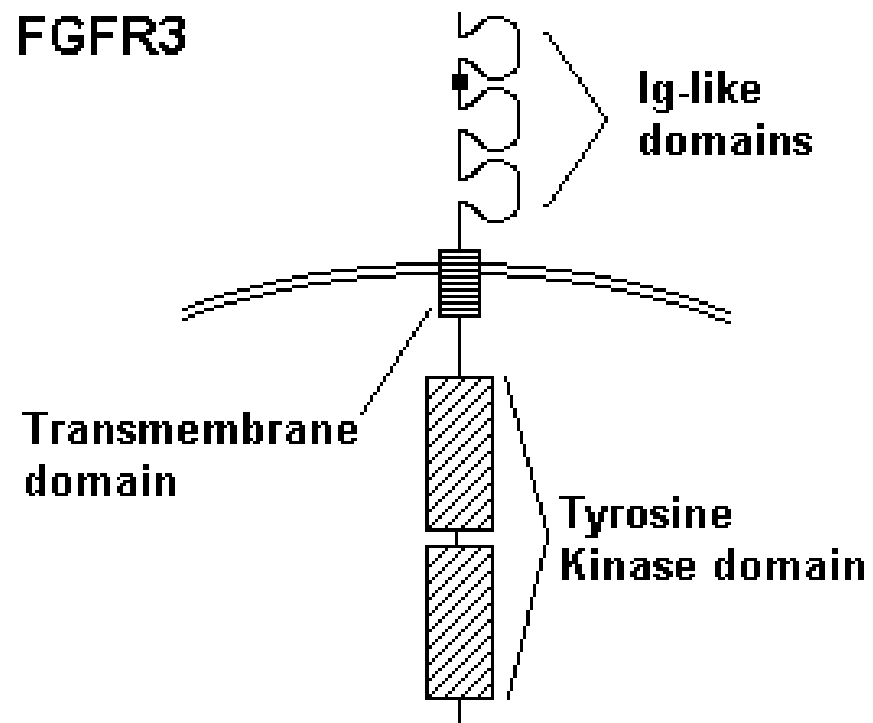


Figure 1. Schematic representation of the FGFR-3 protein. (Modified from Spivak-Kroizman et al. 1994)

To date there are four FGFRs that are now defined and characterized. The four share between 55% and 72% homology at the protein level. (Johnson and Williams 1993) It has also been shown, however, that receptor diversity plays a major role in defining the function of the FGF-FGFR signaling system. The multiple types of FGFs and their wide range effects on target cells demands a diverse system of receptors. For example, FGF-7 elicits a mitogenic response in keratinocytes but not fibroblasts or endothelial cells (Rubinet al. 1989). This led to the belief that the FGF-FGFR signaling system differs between the cell types.

In order to gain the diversity in these cells, as well as other cells expressing FGFRs, it is believed that the receptors use one of two mechanisms, either alternate splicing of the same gene, or analogous splice variants of different genes. In either case, most of these variances occur in the immunoglobulin-like domains or in the tyrosine kinase domains (Johnson and Williams 1993). For instance, FGFR-1 has three possible ends to the IgIII region named IIIa, IIIb, and IIIc. These different ends to the third immunoglobulin-like domain allow the receptor to change its specificity for different FGFs.

Because of the large number of FGFs and the different forms of the FGFRs, there are still many questions as to the exact processes of interaction between the two and how they all interact with each other. It is known, however, that the great diversity in the signal and receptor process is accomplished by different FGFs binding to different FGFR splice variants and different *fgfr* gene products.

The FGF receptor behaves like most other tyrosine kinase receptors to initiate a signal transduction pathway. Binding of FGFs to the extracellular domain of the receptor turns on the catalytic activity of the tyrosine kinase domain on the cytosolic side of the receptor. This is accomplished by FGFR dimerization. When a FGFR receptor is bound

by a FGF, it dimerizes with another FGFR-FGF complex (Plotnikov et al. 1999). The catalytic domain of one receptor complex phosphorylates tyrosine residues on its own catalytic domain and the catalytic domain of the adjacent receptor complex and vice versa (Lemmon and Schlessinger 1994). Autophosphorylation gives the receptor a greater capacity to phosphorylate other targets within the cell. The dimer may consist of FGFRs of the same type, i.e. FGFR1-FGFR1, or the dimer may consist of two different receptors in the same family, i.e. FGFR1-FGFR2 (Bellot et al. 1991). This added variance to receptor function contributes to the wide spectrum of FGF signaling. (Figure 2.)

After the FGFR receptor has become activated, the tyrosine kinase begins activating proteins of the signal cascade by phosphorylation. The most common sites of phosphorylation are Src-homology-2 (SH2) regions on target proteins. Phosphorylation of the target protein usually causes a conformational change that activates various catalytic activities unique to the target. FGF receptors generally activate four different protein pathways to propagate the signal. The first is phosphorylation of the SH2 domain of phospholipase C-gamma (PLC γ) to stimulate activation. Activated PLC γ then goes on to cleave phosphatidyl-inositol-4,5-bisphosphate to inositol triphosphate (IP₃) and diacylglycerol (DAG). IP₃ is then responsible for releasing calcium stores within the cell while DAG and calcium activate protein kinase C, a second messenger protein. The second pathway is to phosphorylate the SH2 domain of the protein Crk which in turn activates other signaling molecules Shc, Cas, and C3G. Crk is an SH2/SH3- containing adaptor protein which helps to link FGFR to other downstream signaling molecules (Larsson et al. 1999). Shc helps to link FGF receptors to the Ras signaling pathway (Yulug et al. 1995). The Cas (cellular apoptosis susceptibility) protein is believed to function in mammalian cells in both apoptosis and cell proliferation (Brinkmann

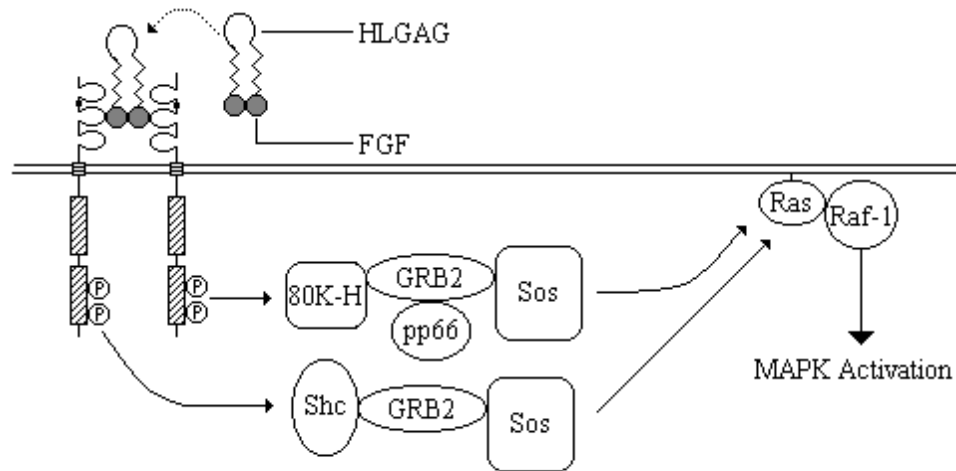


Figure 2. Schematic representation of a dimerized FGFR-3 complex and the phosphorylation of signaling complexes that lead to the activation of the Ras system.

et al. 1996). C3G (guanine nucleotide-releasing protein) is also believed to help transducer signals from tyrosine kinases to the Ras system (Tanaka et al. 1994). The third protein activated using SH2 is the Src protein, which is a membrane bound, non-receptor tyrosine kinase. The Src protein is believed to amplify the original signal. The fourth protein system, the SNT-1/FRS-2 protein is unique in that it does not use SH2. Two independent groups discovered this protein by using mutated FGFRs that did not contain any catalytic tyrosine residues. They found that the FGFR still phosphorylated the SNT-1/FRS-2 protein. This protein, through a series of events, is believed to recruit the Ras protein (Wang et al. 1996, Kouhara et al. 1997). The subject of the FGFRs' signaling system is still largely unknown. The various combinations of FGFs and FGFRs contribute to the complexity of the system and there is a seemingly endless outcome to each signal.

This signaling pathway is heavily dependent on heparin, as mentioned above. Heparin in the pericellular matrix or in transmembrane proteoglycans associates with FGFs and the extracellular surface of the FGFRs, allowing the FGFR signaling complex to recognize changes in its immediate environment (McKeehan et al. 1984). These changes add to the great diversity of the complex signaling system, and heparin is believed to aid in keeping everything organized. Heparan sulfate has also been implicated in many aspects of FGF stability, receptor stability, FGF-FGFR complexes, receptor function, and non-signal stability of the FGF receptor (Luo et al. 1996, Kato et al. 1998, Moy et al. 1997). Heparan is believed to have two major roles in receptor function. The first is to help maintain a general stability over the entire system by divalent cation-dependent high affinity interaction with the FGFRs that help ensure proper binding with FGFs (Kan et al. 1996). The second is to inhibit random receptor dimerization in the absence of FGF. This is achieved because of HLGAGs' (heparin-like glycosaminoglycans) ability to bind to a

specific site on the FGFR protein. This site lies between two immunoglobulin-like domains that when HLGAGs are not bound, tend to favor non-signal dimerization. FGF binding removes the HLGAGs then allowing receptor dimerization (Kan et al. 1996).

CHAPTER 4. FIBROBLAST GROWTH FACTOR RECEPTOR 3

In 1991, Keegan et al., isolated a new human tyrosine kinase receptor cDNA. This cDNA was highly homologous to the previously described FGFRs. This receptor was a 125-kDa glycoprotein that, through calcium efflux studies, was shown to be activated by human FGF-1 and FGF-2. Because of the common attributes shared between this ‘new’ receptor and the other FGFRs, it was given the name FGFR-3. FGFR-3 is made up of three immunoglobulin-like regions, a transmembrane domain, and a cytoplasmic tyrosine kinase receptor. The IgI and IgII domains are separated by an acidic amino acid sequence and the tyrosine kinase domain is split into two parts by a series of 14 amino acids (Figure1.)(Keegan et al. 1991).

Thompson et al. (1991) isolated the FGFR-3 gene from the Huntington’s Disease (HD) region of chromosome 4, p16.3, an area spanning about 2.5 million base pairs. Initial research into the FGFR-3 gene was hoping to point to its site as a possible candidate for the HD gene because of its involvement with growth factors and its map location. This, however, did not prove to be the case.

The FGFR-3 gene contains 19 exons and 18 introns spanning 16.5 kilobases (Perez-Castro et al. 1997). The cDNA consists of 4.4 kb and contains an open reading frame of 2,520 nucleotides. The FGFR-3 protein is made up of 840 amino acids.

FGFR-3 expression is highest during early embryonic development. Most of the activity is seen in the precartilagenous condensing mesenchyme and in bony and cartilagenous structures of the developing vertebrate (Peters et al. 1993). Further on in development it is concentrated in the perichondrium, the resting cartilage, and the

maturation and hypertrophic zones of the growth plate. Here it is believed to play a major role in chondrocyte differentiation.

There are two different isoforms of the FGFR-3 receptors, depending on splice patterns. These two isoforms differ in which third immunoglobulin-like domain is used and are so named FGFR-3 IIIc and FGFR-3 IIIb. The IIIb form was isolated from epidermal keratinocyte cell populations in the mouse skin. The IIIc form was found in nonepithelial cell populations predominantly the brain, spinal cord, and other bony structures in the mouse (Murgue et al. 1994, Keegan et al. 1991). These splice forms not only differ in the tissue in which they are expressed, but also their ligand affinity and preferential ligand binding.

FGFR-3 has been shown to be activated by FGF-1,-2,-4,-8, and -9 (Vajo et al. 2000). The variability of FGFR-3 receptor itself and the number of FGFs that may activate the receptor give the system a high range of possible signals.

Like the other FGFRs, an enormous cascade of events takes place after a ligand has bound to the FGFR-3 receptor. For the most part there are great similarities in all the signaling systems. FGFR-3 primarily links itself to the Ras/MAPK system through a unique interaction between GRB2-nucleotide exchange factor Sos complex and either the Shc protein or the 80K-H protein (Figure 2.)(Kanai et al. 1997). This system has been implicated as a signaling pathway important for growth factor induced cell cycle progression.

Disruption of the FGFR-3 gene in mice was initiated in order to study the specific function of the signaling system. Mice with homozygous disruptions of the FGFR-3 receptor showed enhanced growth of long bones and vertebrae. This suggests that the FGFR-3 gene negatively regulates bone growth (Deng et al. 1996, Colvin et al. 1996).

Fibroblast growth factor receptor 3 (FGFR-3) is perhaps the most well known of the other fibroblast growth factor receptor proteins. Defects in this gene cause a myriad of skeletal dysplasias, i.e. achondroplasia, hypochondroplasia, thanatophoric dysplasia, Crouzon syndrome, Muenke syndrome, and SADDAN dysplasia. The two most common defects, achondroplasia and hypochondroplasia, are the focus of this study.

CHAPTER 5. SKELETAL DYSPLASIAS

5.1 ACHONDROPLASIA

Achondroplasia (ACH) is the most common genetic form of short-limb dwarfism. It is an autosomal dominant trait and occurs between 1 in 15,000 and 1 in 40,000 live births (Jones et al. 1988, Gorlin et al. 1990, Murdoch et al. 1970, Gardner et al. 1977, Oberklaid et al. 1979, Andersen and Hauge 1989, Stoll et al. 1989). There are many phenotypic characteristics of ACH. These include a host of skeletal abnormalities including, but not limited to, rhizomelic dwarfism, relative macrocephaly, exaggerated lumbar lordosis, characteristic facies with frontal bossing and mid-face hypoplasia, limitation of elbow extension, genu varum, trident hand, hyperextension of most joints, and other typical bone abnormalities (Jones et al. 1988). These characteristics contribute to varying expressions of the disease Achondroplasia. An affected individual may have a small or high number of these discernable characteristics. However, these characteristics are obvious and consistent enough to ensure proper clinical diagnoses based on physical observation and radiological techniques at the time of birth.

Histologically, achondroplasia affected individuals show a defect in chondrocyte function during endochondral bone formation. Chondrocytes in the maturing growth plate, specifically the hypertrophic zone, appear to be inhibited during their maturation and development and the frame for matrix calcification is never properly constructed. This severely compromises the length of long bones in the mature individual (Ponseti et al. 1970).

In 1994, the gene responsible for causing achondroplasia was mapped by two groups to the distal 2.5-Mb region of chromosome 4. One group accomplished this by

studying 14 pedigrees while the other used 18 multigenerational families with achondroplasia and 10 short tandem repeat polymorphic markers from this region (Velinov et al. 1994, Francomano et al. 1994). In the same year, the gene causing hypochondroplasia (HCH) was also linked to the short arm of chromosome 4. This study also determined ACH and HCH genetically related (LeMerrer et al. 1994).

These studies pointed to a number of possible genes that might be responsible for ACH. The candidates for the disease included the FGFR-3 gene and because of its known function as a mitogenic receptor, efforts were concentrated on this site. Within six months of mapping the disease to this region of the chromosome, characteristic mutations were documented.

Shiang et al. (1994) and Rousseau et al. (1994) screened the gene for mutations in achondroplastic probands and found a common mutation in the transmembrane coding domain of the gene. In 15 of 16 affected individuals, Shiang found that there was the same G-to-A transition at nucleotide 1138. The mutation of the other individual who did not have the G-to-A transition had a G-to-C transversion at the same nucleotide (Shiang et al. 1994). Both mutations lead to a substitution of an arginine residue for a glycine residue (gly380arg or G380R) at position 380 of the final protein. Concurrently, Rousseau found the same G380R mutation in all cases studied which included 17 sporadic cases and 6 unrelated familial cases (Rousseau et al. 1994).

In a larger study in 1995, Bellus et al. found the G-to-A transition in 150 of 154 unrelated achondroplasia affected individuals, the G-to-C transversion in 3 affected individuals, and in an atypical case an affected individual with out either mutation (Bellus et al. 1995). Additional studies in Sweden, Japan, and China have reported the same G380R mutation (Ikegawa et al. 1995, Alderborn et al. 1996, Wang et al. 1996). Because

of the relatively high occurrence of achondroplasia in the population and the consistency of the mutation, nucleotide 1138 is considered the most mutable nucleotide in the human genome.

The result of a transmembrane mutation in the FGFR-3 has been a vast area of study over the last decade. Previous studies involving mice with disrupted FGFR-3 genes showed that the absence of a properly functioning gene product leads to long bone and vertebrate overgrowth. It could then be inferred that the FGFR-3 receptor is responsible for containing/controlling long bone growth. Because ACH individuals typically have stunted long bone growth and short stature, it can be concluded that the G380R mutation in the transmembrane domain might produce an overly active FGFR-3 receptor, with a gain of function nature that is ligand independent.

This general theory has proved to be the case except for a few minor exceptions. Substitution of a glycine for an arginine in the transmembrane domain of FGFR-3 results in the stabilization and accumulation of mutant receptor at the cell surface. The result is a prolonged period of ligand activated receptor signaling (Monson-Orr et al. 2000). The ligand is needed for over activation of the receptor in achondroplasia but as will be seen later this is not the case for other skeletal dysplasias. Growth is stunted because the extended length of inhibition at the growth plates of long bones slows chondrocyte terminal differentiation.

The process of long bone growth is a highly sensitive series of events that are dependent on coordination and precise balance among chondrocyte proliferation, differentiation, cartilage matrix formation, and mineralization within the growth plate. These events are under a great deal of influence from local and distant signals, such as hormones and fibroblast growth factors. The timing and concentration of these signals are

critical during development. Because of the highly tuned series of event that take place at the growth plate, it becomes very sensitive to even the smallest insults, such as an altered FGFR-3 receptor.

5.2 HYPOCHONDROPLASIA

Hypochondroplasia (HCH) is another genetic disorder of short stature. It was initially described in 1913 but wasn't officially termed and recognized until 1960 (Ravenna et al. 1913, Maroteaux and Lamy 1964). It is very similar to achondroplasia but has a less severe phenotype. General characteristics of HCH share those of ACH and include, but are not limited to, rhizomelic shortening of the limbs, short fingers, megaloccephaly, narrowing of the spinal cord, square and shortened ilia, and shortened tubular bones (Walker et al. 1971). These features do tend to be much milder than those of ACH, though. Hypochondroplasia has a wide range of possible phenotypes, and unlike achondroplasia, the clinical diagnoses and radiological findings may be somewhat vague in pointing to the disease. Hypochondroplasia is therefore addressed on a case by case basis. There has been established, however, a discernable difference between achondroplasia and hypochonroplasia from both clinical and radiological diagnoses. Hypochondroplasia is an autosomal dominant mutation (Beals et al. 1969). It is not as common as ACH, but its rate of occurrence has not yet been calculated. This is due in part to the wide range of phenotypes and the fact that childhood onset of symptoms occurs regularly.

It was theorized that achondroplasia and hypochondroplasia are allelic based on the similarities in phenotype of the two disorders and the identification of a severely dwarfed individual whose father had achondroplasia and whose mother had hypochondroplasia (McKusick et al. 1973). The discovery of the common G1138A/C mutation in the FGFR-3 gene in ACH individuals also encouraged the search for hypochondroplasia to the same

gene. In 1995, Bellus and Prinos located a common mutation in exon 13 of the FGFR-3 gene in HCH individuals. They both discovered an asparagine to lysine substitution at amino acid 540 (asn540lys or N540K) in the final protein (Bellus et al. 1995, Prinos et al. 1995). There was some contradiction in the exact nucleotide number however, Bellus called it a C1620A/G mutation while Prinos, using a different numbering system, called it a C1659A/G mutation. Today it is numbered base 1620. They both mapped it to amino acid 540, though, which is located in the proximal tyrosine kinase domain of the final protein.

ACH and HCH have been separated genetically and there appears to be no crossover of mutations between the diseases. In 1995, Stoilov et al. found the gly380arg mutation in 21 of 23 ACH individuals while the same mutation was not found in any of the 8 HCH individual studied (Stoilov et al. 1995).

The percentage of individuals with this mutation wasn't as high as the 95% of ACH individuals who had the G1138A/C gly380arg substitution. These percentages fell more on the order of about 50% to 70%. Bellus et al. found the C to A mutation in 8 of 14 (57%) individuals and Ramaswami et al. found the same mutation in 28 out of 65 (43%) individuals with hypochondroplasia (Ramaswami et al. 1998). Also in 1998, Fofanova et al. studied 16 individuals and found that 6 had the C to A mutation and 3 had the C to G mutation (56% at nucleotide 1620) (Fofanova et al. 1998). In a study of 18 Taiwanese patients, Tsai et al. found the C to A mutation in 6 patients and the C to G mutation in 4 patients (56% at nucleotide 1620) (Tsai et al. 1999).

Because the C1620A/G mutation did not account for all of the HCH individuals, the FGFR-3 gene was screened for other mutated sites. Novel mutations were found in the FGFR-3 gene of HCH individuals such as ile538val, ans540thr, asn328ile, lys650asn/gln,

and asn540ser (Grigelione et al. 1998, Deutz-Terlouw et al. 1998, Winterpacht et al. 2000, Bellus et al. 2000, and Mortier et al. 2000). These additional mutations have helped to account for most of the mutations in HCH affected individuals, however, there have still been a few HCH individuals who have not had any of these mutations. Overall, this leaves HCH individuals broken into two categories, those with FGFR-3 mutation and those without. A great deal of study has also gone into determining whether or not different mutations may lead to different phenotypes, but this has been a rather daunting undertaking.

Hypochondroplasia has been termed a genetically heterogeneous disease. This is due to the fact that not all of the individuals with the disease carry the same mutation.

Because the HCH N540K mutation lies in the proximal tyrosine kinase domain of the FGFR-3 receptor, it results in functional problems unlike those of mutations in the transmembrane domain. As mentioned previously, transmembrane mutations cause the FGFR-3 receptor to harbor an extended response in the presence of FGF ligands. The tyrosine kinase mutation, however, causes a ligand independent activation of the receptor. The receptor may also become activated without dimerization. A major difference between the two mutations though, is that when a FGF ligand does bind to the receptor, a great deal of wild type FGFR-3 function ensues, thereby possibly negating the mutation (Raffioni et al. 1998). The return of some wild type function may account for the less severe and noticeable phenotype of hypochondroplastic individuals.

Hypochondroplasia presents a wide spectrum of developmental irregularities and skeletal abnormalities. There have been dozens of clinical cases to date of the varying phenotypic degrees of the disease and the mutations that may cause them. The many

different mutations of the receptor and the consequences of the mutations on function are beyond the scope of this thesis.

CHAPTER 6. MUTATIONS AND DISEASE

Advances in molecular genetics over the last two decades have increased our understanding of the origins of genetic mutations. The bulk of these studies, though, have focused on prokaryotic and lesser eukaryotic organisms, such as the fruit fly *Drosophila melanogaster*. However, little has been discovered on the processes of mutation in the human genome. Research has been able to point to mutations causing many genetic diseases, but the actual origin and processes behind these disease causing mutations has yet to be discovered. Achondroplasia and Hypochondroplasia are both genetic diseases whose mutation site is known but the origin of the mutation remains a mystery.

There are many factors that are believed to contribute to the process of mutation. These can be classified as either exogenous or endogenous processes. Exposure to radiation and chemicals that permanently alter the DNA are the two most widely accepted processes for exogenous mutation induction. However, there are mutations that can occur without exposure to harmful radiation or mutagenic chemicals. These endogenous mutations can occur because of an error in proofreading during replication or from a spontaneous occurrence like spontaneous deamination of 5-methylcytosine. These types of mutations can also be referred to as 'spontaneous mutations'. Generally, a spontaneous mutation has come to mean a phenotypic mutation in an offspring that is not evident, at least phenotypically, in the paternal genome.

Spontaneous mutation is generally considered to be harmful to an individual and have deleterious effects. However, mutation is thought to be very beneficial on an evolutionary level and the driving force behind natural selection. Therefore, it would be

advantageous to be able to estimate the rate of spontaneous mutation in the human genome. This would provide some preliminary clues as to the rate of evolution.

Many attempts have been made to correctly calculate the rate of spontaneous mutation in the genomes of many different species. It was discovered that the rates of spontaneous mutation per genome are remarkably similar within broad groups of organisms, but differ greatly among groups. Mutation rates in RNA viruses that contain at least 10^4 bases is about 1 mutation per genome per replication for lytic viruses and about 0.1 mutation per genome per replication for retroviruses. The mutation rate for microbial organisms with DNA based genomes is on the rate of about 1/300 per genome per replication. Mutations in higher eukaryotes have a much broader range, something on the scale of 0.1-100 per genome per sexual generation or per meiotic event (Drake et al. 1998).

The difficulty in understanding the comparison between the different groups of organisms stems from the methods of studying the mutations and the total amount of essential DNA in the organism's genome. Viruses have relatively small genomes when compared to eukaryotes and the bulk of their DNA is essential for proper function and survival of the organism. Studies also measure the rate of mutation based on a rate of phenotypic change. Therefore, a mutation of the virus' DNA in an essential portion of the genome is much more phenotypically relevant than a mutation in the eukaryotic genome in a nonessential region. This fact is one of the major reasons that it has been difficult to accurately extrapolate human spontaneous mutation rates based on studies of lower organisms.

The genetic diseases achondroplasia and hypochondroplasia provide good models by which to study spontaneous mutation. The human genome is relatively large and complex. It contains a relatively small portion of meaningful genetic code. Because of

this it can be assumed that most spontaneous mutations, like single base substitutions, do not result in any phenotypic change. The use of the third base 'wobble' in each codon, in which the third base doesn't account for much difference between amino acids, also helps to mask spontaneous mutations in the human genome. Mutations resulting in amino acid changes in nonessential regions of the protein product may also go unnoticed. Therefore, dominant mutations, especially those with complete penetrance and dramatic phenotypes, like achondroplasia and hypochondroplasia, have served as the main means to study spontaneous mutation in man during this century.

Although the frequency of spontaneous mutations is quite important in understanding the origin of genetic diseases, the cell type and stage of that cell in its development is another significant factor to consider. If a spontaneous mutation occurs in a cell, it is usually not a significant event until that cell has clonally expanded or given rise to the next generation of a germ cell. The function and importance of the cell is also a major consideration. Somatic cells with mutations can go largely unnoticed. Problems arise most often when the mutation confers a replicative advantage to a group of cell, as such is the case with general tumor formation. Germ cells, however, with mutation can pass the mutation on to future offspring. This notion is particularly significant in the male germ cell. A germ cell with a mutation can undergo spermatogenesis and develop into sperm carrying the mutation. More importantly the germ cell can undergo mitosis and clonally expand the mutation among the entire population of germ cells to the point where the majority of sperm produced all carry the same mutation.

As mentioned previously, the deamination of 5-methylcytosine in a germ cell is a process by which a spontaneous point mutation can occur. One of the areas where spontaneous deamination of 5-methylcytosine occurs most frequently in the genome is at

cytosine-guanine (CpG) dinucleotides (Bird 1980). CpG sites are most affected because these cytosine nucleotides, bonded with guanine, have the highest proportion of methylation among the cytosine nucleotides.

Cytosine methylation is a very important signal in normal cellular function. Methylation of various base pairs at these sites helps to create developmental signals on the genome for different enzymes that are active during embryogenesis. Methylation is believed to either turn 'on' or 'off' different genes during development. Methylation is also used as an epigenetic modification marker of parental imprinted genes (Bird 1987).

Deamination of 5-methylcytosine at CpG sites is considered to be one of the major endogenous mechanisms for the induction of spontaneous mutations. Deamination of 5-methylcytosine forms thymidine and generates a G-T mismatch which, if not repaired, produces a C to T transition. Deamination of cytosine can also generate a C to T transition if uracil glycosylase and G-T mismatch repair are inefficient.

Because 5-methylcytosines are so easily mutated, molecular studies of the genome have shown that they are severely underrepresented. They probably are actually represented by a factor of 4 to 5 more than found in the genome (Schorderet and Gartler 1992). This leaves the remaining 5-methylcytosines with an even larger impact on the spontaneous mutation in the human genome. Studies have shown that approximately 37% of all spontaneous germ-line mutations responsible for genetic disease are localized to CpG dinucleotides (Cooper and Youssoufian 1988).

Deamination of 5-methylcytosine appears to be a major factor in the formation of achondroplasia mutations. In almost all cases of achondroplasia, the mutations were spontaneous mutations from glycine to arginine at base site 1138. This guanine is part of a CpG dinucleotide.

It has been accepted for quite some time now that the distribution of the parental origin of germ-line mutation is not equally distributed between the sexes. This became evident in the first studies on hemophilia. Haldane et al. (1947) first reported that there was a higher male than female rate for the origin of mutation in hemophilia families. Lately, molecular genetics has confirmed a sex bias in germ-line mutations. Most studies of the sex ratio for point mutations in hemophilia A and B have shown a greater number of mutations in males (Rosendaal et al. 1990, Sommer and Ketterling 1996). This effect is even more pronounced with respect to point mutations leading to hemophilia at CpG sites, which account for about 40% of all point mutations in hemophilia.

There are three major explanations for the observed sex bias in the origin of spontaneous mutation. The first theory is that if germ-line mutations are assumed to be largely the results of replication errors, then the higher number of mitotic cell divisions in the development of spermatocytes, relative to oocytes, might explain the higher mutability of spermatocytes (Vogel and Motulsky 1997). In females, there are 22 cell divisions before meiosis and two during meiosis, giving 23 chromosome replications in total, because only one replication occurs during two meiotic divisions. The sperm produced by a 40 year old man, however, has gone through 610/23, or more than 25 times as many chromosome replications as an egg (Crow 2000).

A second theory is that there is a difference in the levels of CpG methylation between males and females that might result in sex-specific mutation patterns, particularly a higher rate of mutation among males compared to females (Driscoll and Migeon 1990, Crow 1997). However, studies have shown that while DNA methylation is a major determining factor for recurrent CpG germ-line mutations in individuals with hemophilia

and achondroplasia, the higher mutation rate in the male germ line is apparently not a simple reflection of sex-specific methylation differences (El-Maarri et al. 1998).

The third theory behind an increase in germ-line spontaneous mutations is that there might be a combination of both mechanisms. This would mean that there is a fixation of mutation at 5-methylated CpGs as a result of the increased number of male chromosome replications.

It has been accepted for quite some time now that older parents are at more of a risk of having children with genetic disorders. A great deal of work has gone into studying the changes of reproductive functions, fertility, and genetic risks of ageing women. The best known example of a direct maternal age effect occurs in Down syndrome. This disease occurs as a result of transmission of an extra chromosome 21 at the first meiotic division of the oocyte. Transmission of an extra chromosome, also known as trisomy, is much more common in older age females than males (Hassold 1996). It is estimated that about 0.3% of liveborns have an abnormal number of chromosomes, with the most dominant one being chromosome 21. For trisomy 21, almost all extra chromosomes were of maternal origin. The nondisjunction process leading to an extra chromosome 21 is still largely a mystery, though. With males, trisomies could be easily explained by the larger numbers of replication that each germ cell must go through during spermatogenesis. In females, however, there is no increase in the number of pre-meiotic cell divisions with maternal age. As all the oocyte cell divisions are completed before birth, there is no increase in divisions with postnatal age as with males. One of the proposed reasons for the trisomy is perhaps the increased amount of time the chromosomes are in suspended meiosis during the life of the female.

In contrast to older females, who show a higher amount of chromosome segregation mutations, older males have been shown to have an increased incidence of dominant genetic disorders that result from single point mutations (Vogel and Rathenberg 1975, Risch et al. 1987). Although the number of replications a male germ cell makes during spermatogenesis is an important consideration for the explanation of the paternal age effect, it is probably not all inclusive. If accumulation of mitotic errors was the sole reason for the increased incidence of dominant disorders with advanced paternal age, one would expect a linear increase in the incidence with age. Instead, an exponential increase is observed (Vogel and Rathenberg 1975, Orioliet al. 1995, Crow 1997).

Recent molecular studies have shown that mutations responsible for large numbers of sporadic cases of MEN-2B, Apert syndrome, achondroplasia, Crouzon syndrome and Pfeiffer syndrome occur exclusively on the paternal allele (Carlson 1994, Moloney et al. 1996, Wilkin et al. 1998, Glasser et al. 2000). These diseases are all caused by mutations to genes that code for receptor tyrosine kinase. Specifically, they are recurrent point mutations that cause various amino acid substitutions.

The FGFR-3 gene is especially unique in that it has 7 distinct genetic disorders associated with specific missense mutations occurring in different receptor tyrosine kinase domains (Table 1.) (Figure 3.). The combined incidence of achondroplasia and these 6 other FGFR-3 related disorders is greater than 1 per 10,000 pregnancies. This study focused on two specific point mutations in the FGFR-3 gene which cause Achondroplasia and Hypochondroplasia (Figure 4.).

Because of the large numbers of genetic diseases in the population occur at the FGFR-3 gene, it makes our understanding of the mechanisms behind the origin of these mutations very important. Since it is known that the majority of the mutations behind

achondroplasia and hypochondroplasia originate from spontaneous mutations at the paternal allele, understanding the mechanisms behind germline mutations during spermatogenesis would also be very beneficial.

Table 1. FGFR-3 Missense mutations diseases and the base sites at which they occur and the amino acid substitutions that ensue. The “*” identifies the most common mutations found.

Disease	Mutation	References
Achondroplasia	Y278C (A833G) G380R (G1138A*, G1138C) G375C (G1123T)	Zabel et al. 2000 Shiang et al. 1994 Superti-Fuerga et al. 1995
Hypochondroplasia	N328I (A983T) I538V (A1612G) N540K (C1620A*, C1620G*) N540S (A1619G) N540T (A1619G) K650N (G1950C, G1950T) K650Q (A1948C)	Wiinterpacht et al. 2000 Grigelioniene et al. 1998 Bellus et al. 1996 Mortier et al. 2000 Deutz-Terlouw et al. 1998 Bellus et al. 2000 Bellus et al. 2000
Thanatophoric dysplasia, Type I	R248C (C742T*) S249C (C746G) G370C (G1108T) S371C (A1111T) Y373C (A1118G) J807G/C/R/L/S (T2419A, T2419G, G2420T, A2421T, A2421C)	Tavormina et al. 1995 Tavormina et al. 1995 Tavormina et al. 1995 Tavormina et al. 1995 Rousseau et al. 1996 Rousseau et al. 1996 Bellus et al. 1998
Thanatophoric dysplasia, Type II	K650E (A1948G)	Tavormina et al. 1995
SADDAN syndrome	K650M (A1949T)	Tavormina et al. 1999
Coronal Craniosynostosis syndrome	P250R (C749G)	Bellus et al. 1996
Crouzono-dermo-skeletal syndrome	A391E (C1172A)	Meyers et al. 1996

The objectives of this study were to determine the frequency of achondroplasia and hypochondroplasia causing mutations in samples of human sperm. This would be accomplished by developing an assay that gives the frequency of the base substitution mutations at the two most common sites for achondroplasia and hypochondroplasia, sites

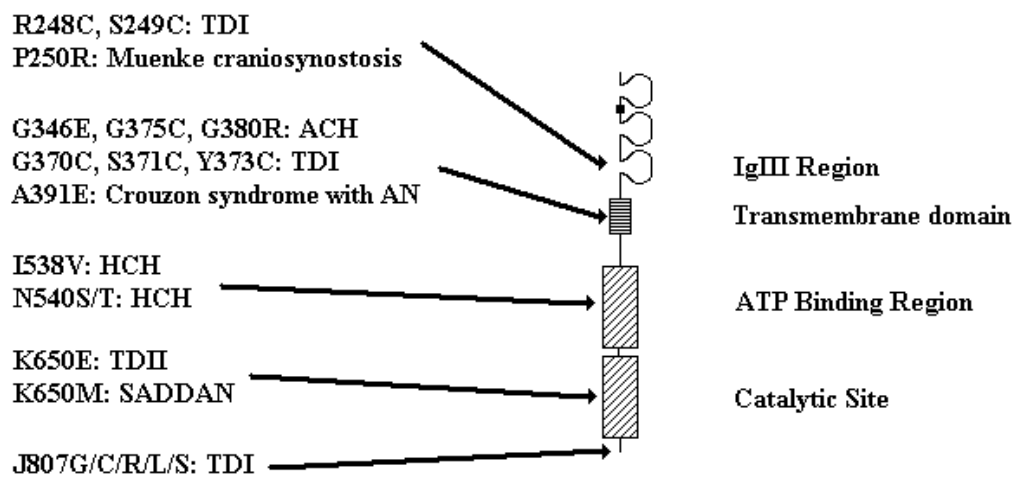


Figure 3. Schematic representation of the FGFR-3 protein and its associated mutations and diseases. TDI, thanatophoric dysplasia type I; ACH, achondroplasia; AN, acanthosis nigricans; HCH, hypochondroplasia; TDII, thanatophoric dysplasia type II; SADDAN, severe achondroplasia with developmental delay and acanthosis nigricans. (Adapted from Vajo et al. 2000)

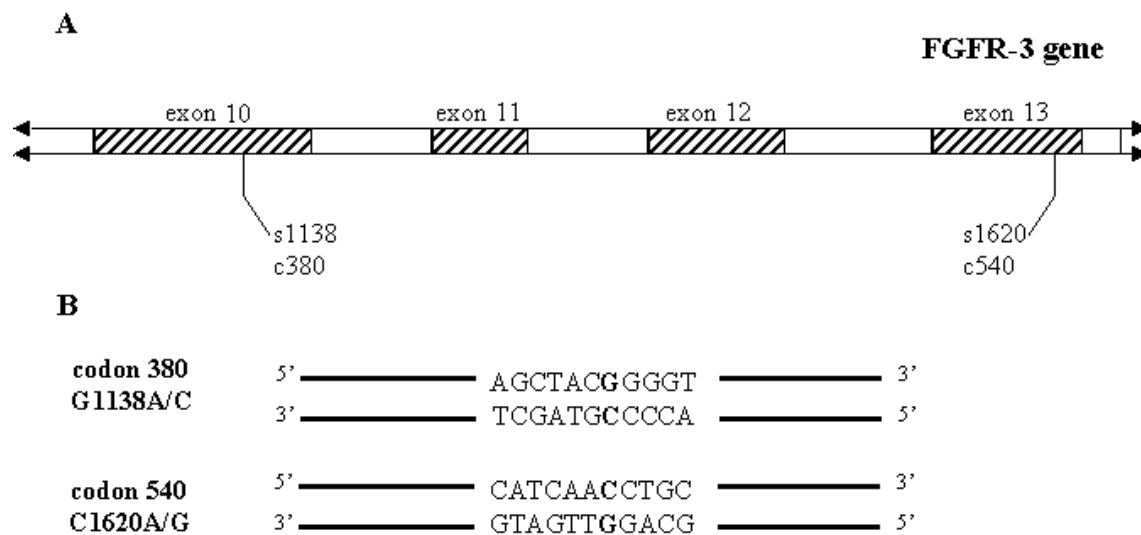


Figure 4. Graphic representation of ACH and HCH mutations. A) Positions of achondroplasia (s1138) and hypochondroplasia (s1620) mutations in the FGFR-3 gene. B) Sequence of nucleotides at the mutation site.

1138 and 1620, respectively. Sperm samples from affected individuals, fathers of affected individuals and normal individuals could then be assayed to determine if the frequency of mutation is higher in any one group.

CHAPTER 7. APPROACH

The purpose of this study was to determine the nature of the spontaneous FGFR-3 mutations that cause Achondroplasia and Hypochondroplasia. This would be accomplished by determining the frequencies of these mutations in sperm samples. With this information, the mechanisms underlying the germline mutations and the possible genetic origin of these diseases may be determined. The hypothesis was that certain gene sequences in the FGFR-3 gene are spermatogenic hotspots for viable disease causing mutations. It was also believed that although the frequency of the mutations might vary, it will still increase with age.

Because both Achondroplasia and Hypochondroplasia are diseases that occur as a result of a single base mutation in the FGFR-3 gene in a single sperm cell, a highly sensitive assay was required to locate the mutation in a large population of sperm cells. For this reason, the Needle-in-a-haystack, polymerase chain reaction/ restriction endonuclease/ ligase chain reaction (PCR/RE/LCR) method of detecting rare mutations was employed (Wilson et al. 1999). This method is based on a selection process that enables a significant increase in the ratio of mutant sequences to wild type sequences. This method has been able to detect single base changes, commonly single base substitution mutations, at a sensitivity of one mutant allele in one cell in up to 10^7 wild type cells.

These Needle-in-a-haystack PCR/RE/LCR mutation detection and identification techniques have enabled the determination of single base changes and the frequencies of these mutations in human and animal tissues (Wilson et al. 1999, 2000, 2001). The frequency of single base mutations in tissue samples can be determined over a range of 10^{-2} to 10^{-7} by adjusting either the amount of sample DNA analyzed by sampling a

consecutively smaller number of genomes or reducing the number of PCR and RE cycles in the selection process.

The approach to the Needle-in-a-haystack assay involved carefully selected nested PCR primer pairs that were used to amplify specific regions of interest, specifically bases 1138 and 1620 (See Figure 4. for reference) of the FGFR-3 gene. At least one primer set overlapped the adjacent intron. This is to ensure that DNA was being amplified from the functional gene, not a pseudogene or RNA. LCR primers were then designed for both mutant and wild type sequences at each specific base site of interest. The LCR primers had discriminating bases at their 3' ends. These primers would only 'match' the template DNA and ligate with the invariant primer if the correct base was in the coinciding spot on the template DNA. By changing the base at the 3' end from C, A, G, or T, the base of the template DNA at the coinciding location could be determined. The Oligo 5.0 software program was used to design primers with T_m values close to 65°C, which is also the optimum temperature for thermostable ligase reactions (Taq ligase). The variable oligonucleotides were designed to have progressively longer 3' poly-A tails, so that they could be separated by size after the ligase reaction on sequencing gels. The invariant primers were labeled on their 5' end with ³²P so that they could be visualized on radiographs. Oligonucleotide mutant standards were used for assay verification and validation.

7.1 APPROACH AT THE HYPOCHONDROPLASIA SITE

The assay for detecting the frequency of Hypochondroplasia causing mutations in the FGFR-3 gene focused on the cytosine at base site 1620. As mentioned previously, this cytosine is substituted with either an adenosine or a guanine changing codon 540 from an asparagine to a lysine (asn540lys or N540K). This base site is located in exon 13 which is

a 111 bp region in the proximal tyrosine kinase domain of the final protein receptor. Primers were designed to flank this region and amplify the mutation with each additional PCR amplification (Table 2.). Table 3 gives the length in base pairs of the PCR products of the various primer sets and the proper annealing temperatures used in the PCR reactions. The restriction digestion with *Bsp*MI (5'-ACCTGC(N)₄-3') was designed to digest the wild type sequences and leave the mutated sequences (5'-ACATGC-3' or 5'-ACGTGC-3'). LCR primers were then designed to detect and amplify the mutations at base number 1620 (Figure 5., Tables 4,5.).

Table 2. Version 1 primer sequences and annealing temperatures for the PCR/RE selection of the C1620A/G base change at codon 540 of the human FGFR3 gene. The bold “T” in the 6th position in primer T represents an incorporated base change designed to eliminate an unwanted *Bsp*MI RE site.

Primer	Sequence	Tm Values
S	5'-GTAGCCGTGAAGATGCTGAAAGGTGAG-3'	73°C
VR	5'-CCAGCCTACTCCACCCACACCTG-3'	74°C
T	5'-GGCGGTCAGGGGTGCAGAG-3'	73°C
WR	5'-GCGGCTTGCAGGTGTCGAAG-3'	74°C
YR	5'-CTCCTCAGACGGGCTGCCAG-3'	73°C

Table 3. Primer sets, annealing temperatures, and PCR product length of the Version 1 PCR protocol for the Hypochondroplasia site.

Primer Set	Annealing Temperatures	PCR Product Length (bp)
S-VR	68°C	521
T-WR	68°C	370
T-YR	68°C	249

7.2 APPROACH AT THE ACHONDROPLASIA SITE

The assay for detecting the frequency of Achondroplasia causing mutations in the FGFR-3 gene focused on the guanine at base site 1138. As mentioned previously, this guanine is substituted with either an adenosine or a cytosine. This substitution changes codon 380, which originally coded for the amino acid glycine, to an arginine residue

Table 4. LCR Version 1 primers and size in base pairs for the Hypochondroplasia site. The bolded bases denote a designed base pair change. The underscored bases in the variant primers indicate the base which must be present at base pair 1620 for ligation to be successful and yield product.

LCR Primer	Size (bp)	Sequence (5' to 3')
Discriminating Set		
Sense Strand		
Mts3TL	30	AAATAAAGGAAACACAAAAACATCATCAAT <u>T</u>
Mts3GL	28	ATAAAAGAAACACAAAAACATCATCAAG <u>G</u>
Mts3AL	26	AAAAAAAACACAAAAACATCATCAAA <u>A</u>
WtFGFR3c540s3L	24	AGGAAACACAAAAACATCATCAAC <u>C</u>
Antisense Strand		
WtFGFR3c540s3LR	18	AAGCAGGAGCCCAGCAGG <u>G</u>
Mts3ALR	20	AAAAGCAGGAGCCCAGCAGT <u>T</u>
Mts3GLR	22	AAAAAAAACAGGAGCCCAGCAGC <u>C</u>
Mts3TLR	24	AAAAAAAAGCAGGAGCCCAGCAGA <u>A</u>
Invariant Set		
FGFR3c540s3L	21	CTGCTGGGCTCCTGCACGCAG
FGFR3c540s3LR	30	TTGATGATGTTTTTGTGTTTCCCGATCATC

Table 5. Sizes of LCR product, from both the sense and antisense strands, for the various wild type (Wt) and mutant (Mt) primers for the Hypochondroplasia site.

DNA Strand	Wt	MtA	MtG	MtT
Sense	45	47	49	51
Antisense	48	50	52	54

(gly380arg or G380R). Primers were designed to flank this region and amplify the mutation with each additional PCR (Table 6.). The primers were also designed to incorporate a *Bsa*II restriction endonuclease site (5'-CCNNGG-3') to allow for digestion of wild type DNA because no restriction enzyme has been found to naturally cut at this sequence. These primers changed the original sequence from 5'-CTACGG-3' to 5'-CCACGG-3' (site 1138 underscored). With this new configuration, a mutation at site 1138 to an adenosine or a cytosine would not allow for digestion by *Bsa*II and only original wild-type DNA would be cut. Because of the requirement to incorporate a restriction site, this protocol called for an initial PCR, followed by restriction endonuclease

Table 6. Version 1 primer sequences and annealing temperatures for the PCR/RE selection of the G1138A/C base change of the human FGFR3 gene. The bolded letters in the primers represent incorporated base changes designed to incorporate a *Bsa*II restriction site and to modify the sequence for controlled nested PCR procedures.

Primer	Sequence	T _m Values
A5	5'-GAGAAGGAAGCTGGTTGTAGATGATGAT GGTGATGGTGTGTATGCAGGCATCCTCA GCCAC-3'	71°C
SR	5'-TGGGGGAGCACAGTCCTTTCTTGG -3'	73°C
N2	5'-GAGAAGGAAGCTGGTTGTAGATGATGAT GGTGATGG -3'	69°C
PR	5'-GCAGGCGGCAGAGCGTCA -3'	75°C
YR2	5'-GTCACAGCCGCCACCACCAGGATGA -3'	68°C

Table 7. Primer sets, annealing temperatures, and PCR product length of the achondroplasia site G1138A/C protocol.

Primer Set	Annealing Temperatures	PCR Product Length (bp)
A5-SR	69°C	151
N2-PR	65°C	108
N2-YR2	65°C	94

Table 8. LCR assay for the achondroplasia site 1138 primers and size in base pairs. The bolded bases denotes a designed base pair change. The underscored bases in the variant primers indicate the base which must be present at base pair 1138 for ligation to be successful and yield product.

LCR Primer	Size (bp)	Sequence (5'to 3')
Discriminating Set		
Sense Strand		
MtCL3	22	AAAAATGGCATCCTCAGCCACC <u> </u>
MtTL3	20	AAATGGCATCCTCAGCCACT <u> </u>
MtAL5	16	AGCATCCTCAGCCACA <u> </u>
WtFGFR3G1138L4	19	ACAGGCATCCTCAGCCAC <u> </u> G
Antisense Strand		
WtFGFR3G1138LR3	21	ATTAAGGAAGAAGCCCCACCC <u> </u>
Mt3ALR4	19	TATAGAAGAAGCCCCACCC <u> </u> T
Mt3TLR2	24	ATAATTAAGGAAGAAGCCCCACCCA <u> </u>
Mt3CLR2	26	AAATAATTAAGGAAGAAGCCCCACCC <u> </u> G
Invariant Set		
FGFR3G1138L2	25	GGGTGGGCTTCTTCCTGTTTCATCCT
FGFR3G1138LR3	26	GTGGCTGAGGATGCCTGCATACACAC

(RE) digestion. LCR primers were then designed to detect and amplify the mutations at base number 1138 (Tables 8, 9.).

Table 9. Sizes of LCR product, from both the sense and antisense strands, for the various wild type (Wt) and mutant (Mt) primers for the achondroplasia site 1138.

DNA Strand	Wt	MtA	MtT	MtC
Sense	44	41	45	47
Antisense	47	45	50	52

CHAPTER 8. MATERIALS AND METHODS

8.1 NEEDLE-IN-A-HAYSTACK ASSAY

- **Enzymes**

The Taq polymerases were purchased from Perkin-Elmer/Applied Biosystems (Foster City, CA). The LCR amplification enzyme was purchased from New England Biolabs (Beverly, MA). The restriction endonucleases *Bsp*MI, *Msp*I, and *Bsa*II were also purchased from New England Biolabs. T4 polynucleotide kinase, for end-labeling, was purchased from New England Biolabs.

- **Oligonucleotides and radioactive isotopes**

Oligonucleotide PCR and LCR primers were custom synthesized by BioServe Biotechnologies (Laurel, MD). [α - 32 P] ATP Redivue (>5000 Ci/mmol) was obtained from Amersham (Arlington Heights, IL).

- **Mutant and Genomic DNA**

Human genomic DNA, at a concentration of 0.2 μ g/ μ l, was purchased from Boehringer Mannheim (Indianapolis, IN). Mutant heterozygous DNA was obtained from Dr. Gary Bellus (University of Colorado Health Sciences Center, Denver, CO). Mutant DNA came in concentrations of 200 and 25 ng/ μ l. Samples of the G1138A and G1138C achondroplasia mutations were provided. Samples of the C1620A or C1620G hypochondroplasia mutations were also provided.

8.2 HYPOCHONDROPLASIA SITE

8.2.1 Mutant PCR and Restriction Endonuclease (PCR/RE) Selection of the Hypochondroplasia Site

Six μg of genomic DNA was combined with 6ng (10^{-3}), 60 pg (10^{-5}), or 6 pg (10^{-6}) of mutant DNA. The combined DNA was then digested overnight with *Bsp*MI according to manufacture's recommendations in a minimum volume of 10 μl .

Proper amounts of commercial PCR buffer, MgCl, distilled water, nucleotides, and PCR primer were then added to create a PCR readied solution with the total volume brought to 50 μl . The samples were then subjected to PCR amplification for 25 cycles using the appropriate primers and annealing conditions (Primer set S-VR (521bp); 94°C for 10 minutes to denature, 25 cycles of 1 minute 94°C denature, 1 minute 68°C annealing, and 1 minute 72°C extension, and finished with 10 minutes at 72°C). PCR amplification was accomplished with the Perkin-Elmer 9700 instrument using 1U AmpliTaq Gold (Perkin-Elmer) polymerase activity. 20 μl of the PCR reaction was then digested with *Bsp*MI for up to 12 hours or overnight under the manufacturer's specifications.

Two microliters of the restriction endonuclease digestion reaction was then subjected to a second PCR amplification using nested primers and the appropriate annealing conditions (Primer set T-WR (370bp); 94°C for 10 minutes to denature, 20 cycles of 1 minute 94°C denature, 1 minute 68°C annealing, and 1 minute 72°C extension, and finished with 10 minutes at 72°C). The same restriction digestion was performed on 20 μl of the second PCR solution as per manufacture's recommendations.

Two microliters of the second digestion solution was then subjected to another nested PCR (Primer set T-YR (249bp); 94°C for 10 minutes to denature, 20 cycles of 1 minute 94°C denature, 1 minute 68°C annealing, and 1 minute 72°C extension, and finished with 10 minutes at 72°C). A third and final digestion was performed on the

samples. A total of 3 restriction endonuclease digestions and three PCR amplifications for a total of 65 cycles were performed on the samples prior to LCR analysis.

8.2.2 LCR and PAGE of the Hypochondroplasia Site

After the third and final restriction endonuclease digestion, 1 μ l of the sample was combined with 10-15 U *Taq* DNA ligase, 1 million cpm of 32 P end-labeled invariant primers, 1 μ M of each wild type or each mutant discriminating primer (or a mixture of all the discriminating primers, each at 1 μ M concentration), 4 μ g sheared salmon sperm, in ligase buffer to a volume of 10 μ l containing 20 mM Tris-HCl (pH 7.6), 100 mM KCl, 10 mM $MgCl_2$, 1 mM EDTA, 10 mM dithiothreitol, 1 mM NAD^+ , and 0.1% Triton X-100. Refer to Tables 4 and 5 for the sequences of the individual primers and LCR product size. The LCR process was a two-temperature process using 94°C for denaturation and 65°C for ligation. The resulting ligation products were resolved on a 7 M urea, 10% acrylamide sequencing gel. The gel was then dried for approximately 40 minutes and exposed to x-ray film for 15-60 minutes.

8.3 ACHONDROPLASIA SITE

8.3.1 Mutant PCR and Restriction Endonuclease (PCR/RE) Selection of the Achondroplasia Site

This protocol begins with a PCR amplification to incorporate the proper sequence for the *Bsa*II restriction endonuclease. Either 6 or 60 μ g of genomic DNA was combined with 6ng (10^{-3}), 60 pg (10^{-5}), or 6 pg (10^{-6}) of mutant DNA.

Proper amounts of commercial PCR buffer, $MgCl_2$, distilled water, nucleotides, and PCR primer were added to bring the total volume to 50 μ l. The samples were then subjected to PCR amplification for 25 cycles using the appropriate primers and annealing conditions (primer set A5-SR; 94°C for 10 minutes to denature, 25 cycles of 1 minute

94°C denature, 1 minute 65°C annealing, and 1 minute 72°C extension, and finished with 10 minutes at 72°C). PCR amplification was accomplished with the Perkin-Elmer 9700 instrument using 1U AmpliTaq Gold (Perkin-Elmer) polymerase activity. 20 µl of the PCR reaction was then digested with *Bsa*II for up to 12 hours under the manufacturer's specifications.

Two microliters of the restriction endonuclease digestion reaction was then subjected to a second PCR amplification using nested primers and the appropriate annealing conditions (primer set N2-PR; 94°C for 10 minutes to denature, 20 cycles of 1 minute 94°C denature, 1 minute 65°C annealing, and 1 minute 72°C extension, and finished with 10 minutes at 72°C). The same restriction digestion was performed on 20 µl of the second PCR solution as per manufacture's recommendations.

Two microliters of the second digestion solution was then subjected to another nested PCR (primer set N2-YR2; 94°C for 10 minutes to denature, 20 cycles of 1 minute 94°C denature, 1 minute 69°C annealing, and 1 minute 72°C extension, and finished with 10 minutes at 72°C). A third and final digestion was performed on the samples.

A total of 3 restriction endonuclease digestions and three PCR amplifications for a total of 65 cycles were performed on the samples prior to LCR analysis.

8.3.2 LCR and PAGE of the Achondroplasia Site

After the third and final restriction endonuclease digestion, 1 µl of the sample was combined with 10-15 U *Taq* DNA ligase, 1 million cpm of ³²P end-labeled invariant primers, 1 µM of each wild type or each mutant discriminating primer (or a mixture of all the discriminating primers, each at 1 µM concentration), 4 µg sheared salmon sperm, in ligase buffer to a volume of 10 µl containing 20 mM Tris-HCl (pH 7.6), 100 mM KCl, 10 mM MgCl₂, 1 mM EDTA, 10 mM dithiothreitol, 1 mM NAD⁺, and 0.1% Triton X-100.

Refer to Tables 8 and 9 for the sequences of the individual primers and LCR product sizes. The LCR process was a two-temperature process using 94°C for denaturation and 65°C for ligation. The resulting ligation products were resolved on a 7 M urea, 10% acrylamide sequencing gel. The gel was then dried for approximately 40 minutes and exposed to x-ray film for 15-60 minutes.

CHAPTER 9. RESULTS

9.1 Results of the PCR/RE/LCR of the Hypochondroplasia Site

During the preliminary primer check for PCR and restriction endonuclease reliability of this assay, it was discovered that in addition to the *BspMI* restriction site at codon 540, there were three other restriction sites within the amplified region of the DNA. Since these restriction sites yielded fragmented DNA after the digestions that could not be amplified in the ligase chain reaction, new primer sequences were designed. These second version primers were then used in the same manner as previously described for the first version (First PCR set, S-ZR; Second PCR set, T-ZR; Third PCR set, U-YR) (Table10.).

Table 10. Version 2 primer sequences and annealing temperatures for the PCR/RE selection of the C1620A/G base change at codon 540 of the human FGFR3 gene. The bolded “A” in primer ZR and the bolded “T” in primer T represent an incorporated base change designed to eliminate any unwanted primer/dimer formations.

Primer	Sequence	Annealing Temperature
S	5'-GTAGCCGTGAAGATGCTGAAAGGTGAG-3'	73°C
ZR	5'-GTTACCCTTGGCAGCGTACTCCACCA-3'	78°C
T	5'-GGCGGTCAGGGGTGCAGAG-3'	73°C
U	5'-TGCACAGACGATGCCAACTGACAAG-3'	75°C
YR	5'-CTCCTCAGACGGGCTGCCAG-3'	73°C

Another problem was then encountered with the second version primer set. Digestion of the PCR product was highly inefficient with *BspMI* (Figure 6.). It was estimated that restriction only reached approximately 25%. This inefficiency in digestion was unacceptable if maximum sensitivity of the needle-in-a-haystack protocol was to be attained.

It has been noted that the *BspMI* restriction enzyme can produce inefficient digestion at resistant DNA sequences (Oller et al. 1991). The use of additional cleavable DNA or spermidine has been shown to be able to boost efficiency to acceptable levels. For

this assay, spermidine and ϕ X174 DNA were added separately and together to the PCR mixtures before restriction endonuclease digestion. Spermidine was added at concentrations between 0.5 and 3.0 mM to the digestion reactions. ϕ X174 DNA was added at a concentration between 0.14 and 1.4 nM. Neither of these techniques helped to increase the efficiency of the digestion reaction (Figures 7, 8.).

Since LCR depends on a successful selection process, multiple attempts were made to refine the second version digestion protocol. Multiple combinations of spermidine and ϕ X174 DNA concentrations were added to the reaction mixtures to try and increase digestion product. Increased concentrations of enzyme as well as increased lengths of time were also used to try and increase efficiency. Neither technique was able to increase the efficiency of restriction with *Bsp*MI (Figure 8.).

In conjunction with the PCR and RE trials, initial steps were taken to refine the LCR technique for site 1620. Figure 9 shows the successful LCR product formation with wild-type DNA and standard mutant DNA templates. The wild-type DNA was PCR product from primer set U-YR. The bands on the PAGE gel only represent the sense strands but further adjustments would have produced both sense and antisense bands (See Table 5 for appropriate sizes of LCR product).

9.2 Incorporation of a *Msp*I Restriction Site

It was finally determined that the *Bsp*MI would fail to ever give the desired digestion efficiency. A new set of primers were then developed to incorporate a *Msp*I restriction endonuclease site at codon 540 (Table 11.). In order to accomplish this, the downstream primer of the first set was designed to alter the sequence at codon 541 from 5'-CTG-3' to 5'-CGG-3'. This would give a new sequence of 5'-AACCGG-3' at codons

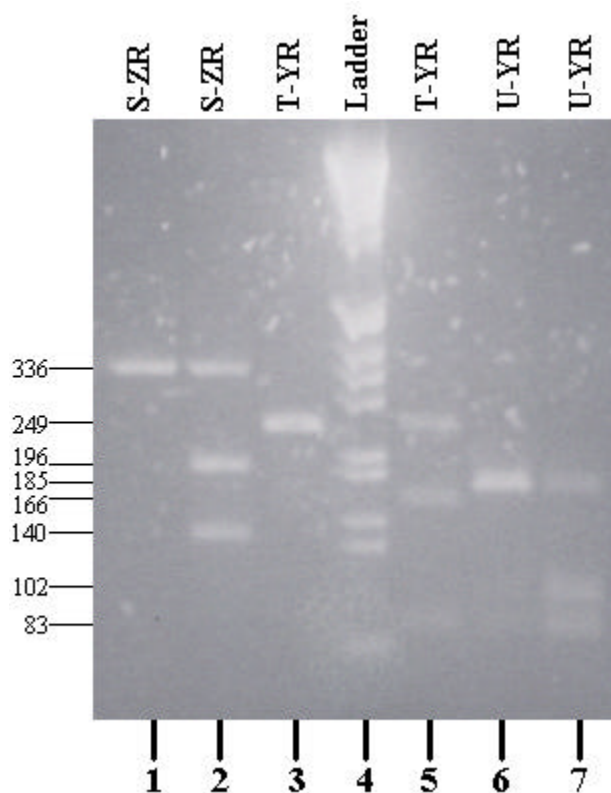


Figure 6. Agarose gel of the PCR products and restriction products of the three PCR primer sets comparing the efficiency of restriction of *BspMI* based on time. Lane 1 – S-ZR at 1 hour. Lane 2 – S-ZR at 24 hours. Lane 3 – T-YR at 1 hour. Lane 4 – DNA Ladder. Lane 5 – T-YR at 24 hours. Lane 6 – U-YR at 1 hour. Lane 7 – U-YR at 24 hours. Results show a moderate increase in efficiency with a longer time for restriction.

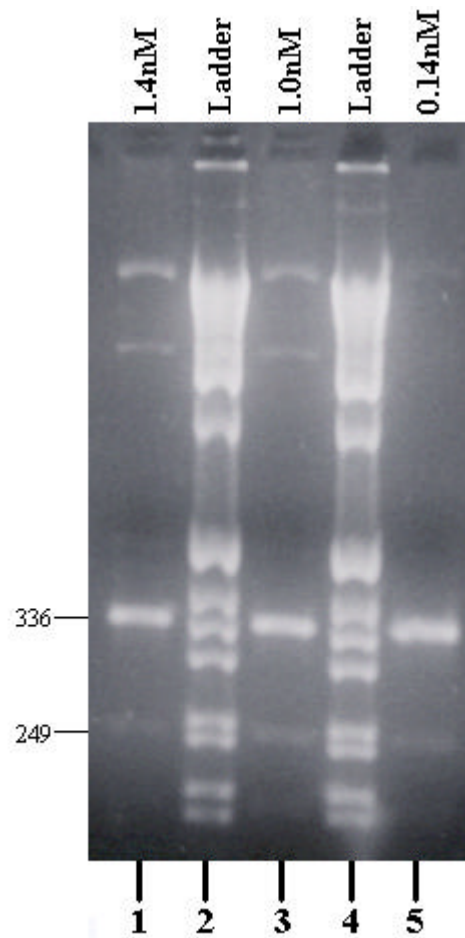


Figure 7. Agarose gel of the PCR products of primer set S-ZR with restriction with *Bsp*MI and the addition of ϕ X174 DNA to increase efficiency. Lane 1 – 1.4 nM ϕ X174 DNA. Lane 2 – HiLo Ladder. Lane 3 – 1.0 nM ϕ X174 DNA. Lane 4 – HiLo Ladder. Lane 5 - 0.14 nM ϕ X174 DNA. Results showed no increase in efficiency with the addition of ϕ X174 DNA. (The bands in the top of the PCR product lanes are restriction remnants of ϕ X174 DNA).

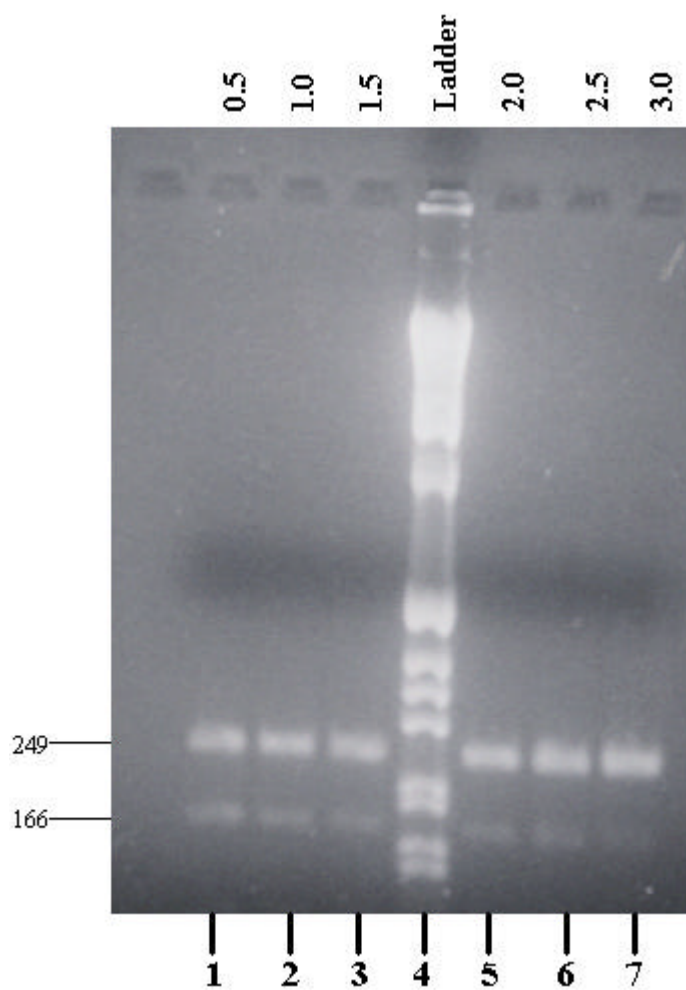


Figure 8. Agarose gel of the PCR products of primer set T-YR with restriction with *Bsp*MI and the addition of spermidine to increase efficiency. Lane 1 – 0.5 mM spermidine. Lane 2 – 1.0 mM spermidine. Lane 3 – 1.5 mM spermidine. Lane 4 – DNA Ladder. Lane 5 – 2.0 mM spermidine. Lane 6 – 2.5 mM spermidine. Lane 7 – 3.0 mM spermidine. Results showed no increase in efficiency with the addition of spermidine.

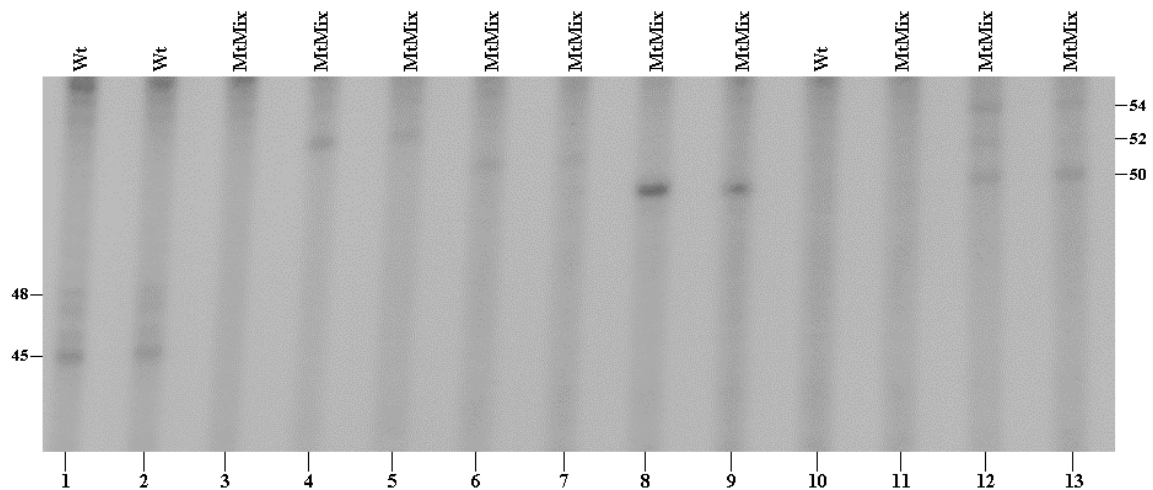


Figure 9. Autoradiograph of a first version LCR testing the Wt and Mt primers and oligonucleotide standards. Primers used are listed at the top of each lane. The template used in each lane is as follows: Lane 1 – Human genome DNA (HG). Lane 2 – HG. Lane 3 – HG. Lane 4 – Oligonucleotide T mutation standard (TLstd) (1pm). Lane 5 – TLstd (0.025pm). Lane 6 – Oligonucleotide A mutation standard (ALstd) (1pm). Lane 7 – ALstd (0.025pm). Lane 8 – Oligonucleotide G mutation standard (GLstd) (1pm). Lane 9 – GLstd (0.025pm). Lane 10 – Blank. Lane 11 – Blank. Lane 12 – Standard mix (1pm). Lane 13 – Standard Mix (0.025pm).

540 and 541 (codon 540 underlined) at which *MspI* would then digest the wild-type sequences.

It should also be noted that several mismatches were incorporated into primers MspIR and ZR2. If successful incorporation of an *MspI* restriction site occurred with primers MspIR and S, then these mismatched bases would also be incorporated into the PCR product. The same sequence of incorporated base pairs was created in primer ZR2, the downstream primer of the second PCR. Thus, only DNA with the proper *MspI* restriction site would serve as template for the second PCR. Figure 10 shows a schematic of the PCR and restriction endonuclease selection process for site 1620.

Table 11. Version 3 primer sequences and annealing temperatures for the PCR/RE selection of the C1620A/G base change at codon 540 of the human FGFR3 gene. The bolded bases in primer MspIR and in ZR2 represent mismatch pairs with the wild type DNA incorporated in order to restrict the template for the second PCR to be limited to first PCR product that had inserted the correct *MspI* sequence.

Primer	Sequence	Annealing Temperature
S	5'-GTAGCCGTGAAGATGCTGAAAGGTGAG-3'	73°C
MspIR	5'-CAGTAGTCGGGTAA TGGATGTAGTGCCCTG CGTGCAGGAGCCCAGCCG-3'	72°C
T	5'-GGCGGTCAGGGGTGCAGAG-3'	73°C
U	5'-TGCACAGACGATGCCAACTGACAAG-3'	75°C
ZR2	5'- G TAGTCGGGTAA TGGATGTAGTGC -3'	64°C

Figure 11 shows the agarose gel of successful sequential PCR selection processes. Primer pairs S-MspIR gave a 239 base pair product, primer pairs T-ZR2 gave a 206 base pair product, and primer pair U-ZR2 gave a 141 base pair product. *MspI* was also able to give efficient restriction at the incorporated site.

The PCR primers were then tested on human mutant C1620G and C1620A DNA. Figure12 gives the Agarose gel of successful PCR (primer set S-MspIR) and restriction with *MspI*. The restriction of the mutant PCR product shows only about 50% efficiency.

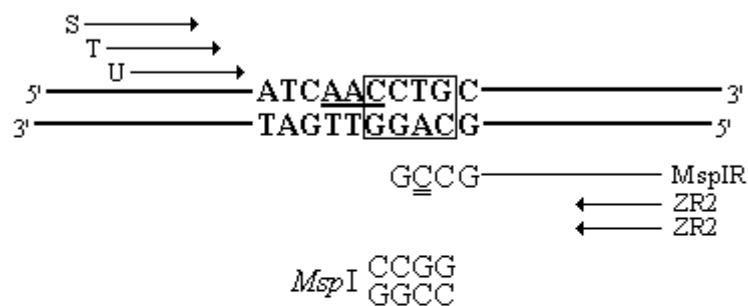


Figure 10. Schematic representation of the incorporation of the restriction endonuclease recognition sequence 5'-CCGG-3' for *MspI*. The first PCR uses primer set S-*MspIR* to incorporate the *MspI* recognition sequence and produce a 239bp product. The second nested PCR uses primer set T-ZR2 to produce a 206bp product. Primer ZR2 is specific for DNA template which has incorporated the *MspI* recognition sequence. The third nested PCR uses primer set U-ZR2 to produce a 141bp product. The box represents the DNA sequence that was altered to incorporate the recognition sequence for *MspI*.

This is a good result because of the nature of the hypochondroplasia mutation. Since hypochondroplasia is a heterozygous dominant mutation (paternal allele), half of the PCR product representing the paternal allele would be mutated and resist restriction and half of the product representing the maternal allele would be wild-type and succumb to restriction.

Since all of the PCR primers were showing proper function, and the *MspI* restriction enzyme was giving efficient restriction, the LCR assay was then designed to accompany this new set of PCR primers.

9.3 Design of the Second Version of the LCR Assay at Site 1620

Because new sequences were incorporated into what would be the template for the LCR procedure, new LCR primers were designed to comply with these changes. Table 12 gives the new discriminating sense and antisense primers as well as the invariant primers. It should be noted that the discriminating sense strand primers did not change with the new set. Figure 13 gives a schematic of the new LCR procedure. The oligonucleotide standards were not changed to carry the 'G' and 'T' changes that were incorporated into the product DNA during the PCR amplification with the *MspIR* primer.

9.4 LCR Results for Site 1620

Figure 14 gives the results of the first attempt to determine the compatibility of the LCR primers with various PCR products. The results showed that the wild-type LCR primers will produce both sense and antisense products with wild-type DNA as the template. There was, however, some contamination with extra bands between the sense and antisense strands. This is not unusual with the amount of PCR/RE primers, enzymes, and reagents that have accumulated during the first steps. It was also determined that the mutant LCR primers both by themselves and in a mix would not form product with wild-

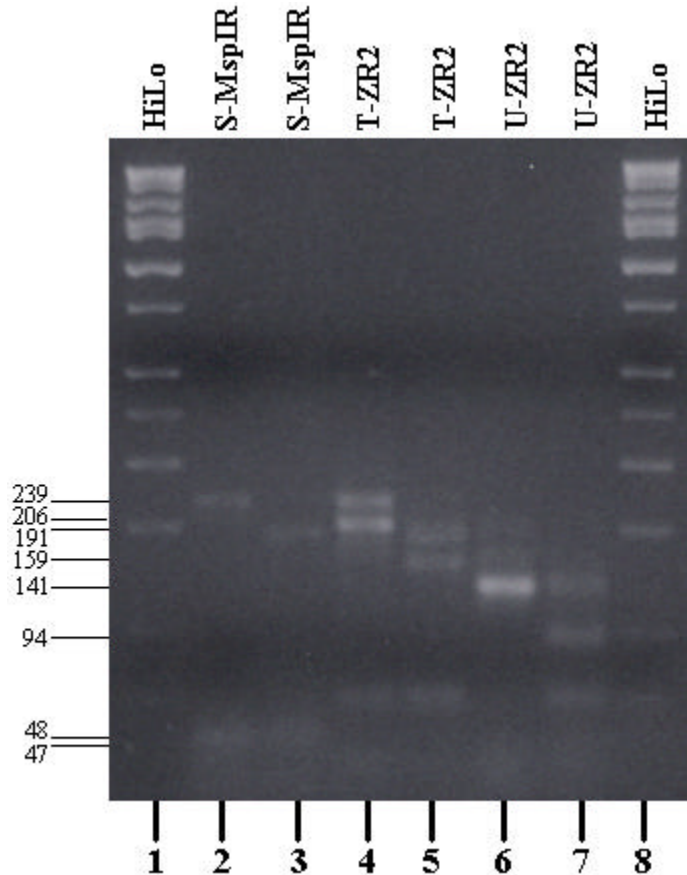


Figure 11. Agarose gel of successful nested PCR/RE sequences. Lane 1- HiLo Ladder. Lane 2 – PCR product with S-MspIR of human genomic DNA. Lane 3 – Restriction of product from Lane 1 with *MspI*. Lane 4 – PCR of product from Lane 3 with primer set T-ZR2. Lane 5 - Restriction of product from Lane 4 with *MspI*. Lane 6 - PCR of product from Lane 5 with primer set U-ZR2. Lane 7 – Restriction of product from Lane 6 with *MspI*. Lane 8 – HiLo Ladder. The 239bp PCR product in Lane 4 can be attributed to left over primers in subsequent reactions. It should also be noted that the increasing intensity around the 50bp size range in Lane 4 and on can be attributed to the build up of the MspIR primer (49mer) and small fragment digestion product of T-ZR2 (48bp) and U-ZR2 (48bp).

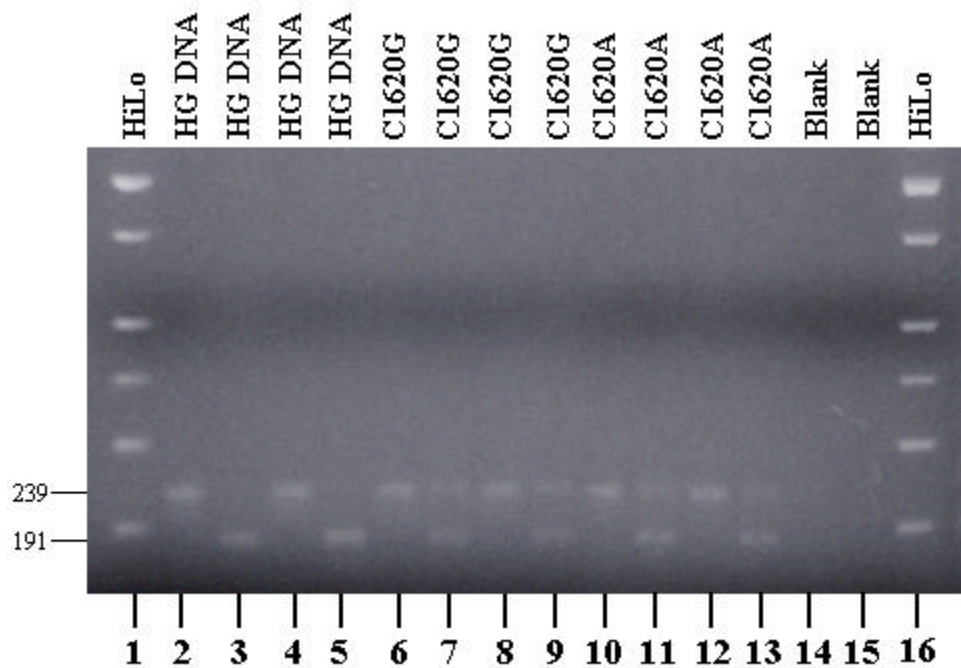


Figure 12. Agarose gel of successful PCR with primer set S-MspIR on wild-type human genomic DNA and human mutant C1620G and C1620A with subsequent restriction with *MspI*. Lane 1- HiLo Ladder. Lane 2 – Human genomic DNA. Lane 3 – restriction of Lane 2 product. Lane 4 – Human genomic DNA. Lane 5 – restriction of Lane 4 product. Lane 6 – Mutant C1620G DNA. Lane 7 – restriction of Lane 6 product. Lane 8 – Mutant C1620G DNA. Lane 9 – restriction of Lane 8 product. Lane 10 – Mutant C1620A DNA. Lane 11 – restriction of Lane 10 product. Lane 12 – Mutant C1620A DNA. Lane 13 – restriction of Lane 6 product. Lane 14 – Blank DNA. Lane 15 – restriction of Lane 14 product. Lane 16 – HiLo Ladder.

Table 12. LCR Version 2 primers and size in base pairs. The bolded bases denote a designed base pair change to coincide with the incorporated base pair changes from the PCR/RE series. The underscored bases in the variant primers indicate the base which must be present at base pair 1620 for ligation to be successful and yield product.

LCR Primer	Size (bp)	Sequence (5' to 3')
Discriminating Set		
Sense Strand		
Mts3TL	30	AAATAAAGGAAACACAAAAACATCATCAAT <u>T</u>
Mts3GL	28	ATAAAAGAAACACAAAAACATCATCAAG <u>G</u>
Mts3AL	26	AAAAAAAACACAAAAACATCATCAA <u>A</u>
WtFGFR3c540s3L	24	AGGAAACACAAAAACATCATCAAC <u>C</u>
Antisense Strand		
WtFGFR3c540s3LR2	18	AAACAGGAGCCCAGCCG <u>G</u>
Mts3ALR2	20	AAAAACAGGAGCCCAGCCG <u>T</u>
Mts3GLR2	22	AAAAAAAAGGAGCCCAGCCG <u>C</u>
Mts3TLR2	24	AAAAAAAACAGGAGCCCAGCCG <u>G</u>
Invariant Set		
FGFR3c540s3L2	21	CGGCTGGGCTCCTGCACGCAG
FGFR3c540s3LR2	33	TTGATGATGTTTTTGTGTTTCCCGATCATCTTC

Table 13. Sizes of LCR product, from both the sense and antisense strands, for the various wild type (Wt) and mutant (Mt) primers for the second LCR design.

DNA Strand	Wt	MtA	MtG	MtT
Sense	45	47	49	51
Antisense	51	53	55	57

type DNA as the template. Both of these results were good in that the assay would probably not produce false positives in the presence of wild-type DNA.

However, this attempt at forming product with mutant primers using mutant oligonucleotide standards (at 1 picomole per reaction) as LCR templates proved unsuccessful. It should also be noted that the mutant oligonucleotide standards did not carry the 'G' and 'T' changes that were incorporated into the LCR mutant primers to coincide with the base changes produced in the template DNA during the PCR process. The DNA used here for template (except for the standard oligonucleotides) was produced

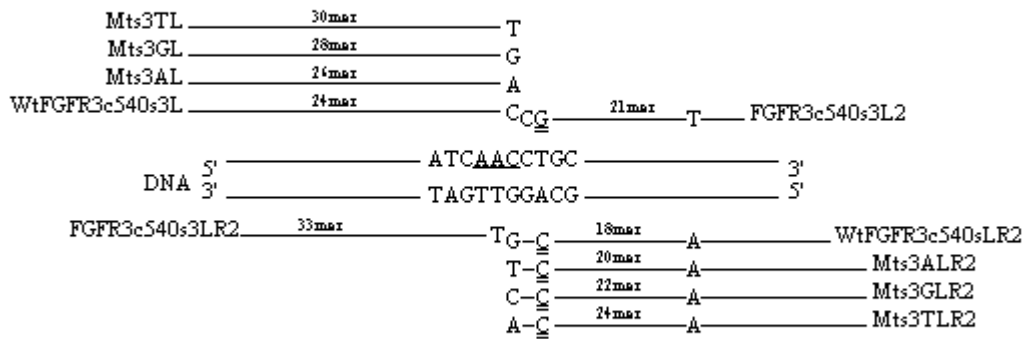


Figure 13. LCR primer design for the detection of mutated sequences in the third base of codon 540. The invariant FGFR3c540s3LR2 and FGFR3c540s3L2 primers as well as the discriminating WtFGFR3c540s3L and WtFGFR3c540sLR2 primers, are complementary to the wild type sequence. These primers will amplify the wild type product using the wild type template in the LCR. Primers Mts3GL and Mts3GLR2, Mts3AL and Mts3ALR2 are complimentary to the N540K mutation (AAC to AAG and AAC to AAA respectively). Primers Mts3TL and Mts3TLR2 would amplify and ligate a thymine inserted at the third spot, not a known mutation, but a primer to be used as a control. These primers will ligate to the invariant FGFR3c540s3L2 and FGFR3c540s3LR2 only in the presence of template DNA containing the appropriate mutation. LCR product fragment sizes are listed in Table 13.

from human genomic DNA with the second nested PCR (primers T-ZR2), after restriction following the first PCR. The first PCR (primer set S-MspIR) used 200ng of wild-type human genomic DNA.

Because the mutant standard oligonucleotide did not ligate successfully, the focus was turned to refining the efficiency of mutant primers ligating with oligonucleotide standards as the template. The concentration of the standard was decreased from 1 picomole to 0.025 picomoles per reaction. This again, however, was not successful in producing ligation. Figure 15 gives these results. Figure 15 also shows the first attempt to form LCR product using human mutant DNA (both the C1620G and C1620A mutations after the second nested PCR (T-ZR2) without restriction) as template with mutant primers. The first PCR (primer set S-MspIR) used 200ng of mutant human genomic DNA for both the C1620G and the C1620A mutations. The mutant primers were unsuccessful in forming product with the mutant DNA. The LCR reaction itself was not the problem in this run because of the positive results with wild-type DNA and wild-type primers and the negative result with mutant and wild-type primers without DNA.

Figure 16 gives the results of an attempt to refine the actual LCR reaction. The ligation reaction was run at a temperature of 64°C instead of the standard 65°C. Lowering the reaction temperature, while increasing the potential for increased ligation, has the tendency to create increased false positives. The DNA used to test the wild-type primers was PCR product made with the third set of primers U-ZR2 on human genome DNA (PCR product was not restricted between PCR sets; they were only sequential nested PCRs). The first PCR (primer set S-MspIR) used 200ng of wild-type human genomic DNA. Wild-type primers were successful in giving sense product (45bp) and antisense product (51bp) showing that the reaction could work with these primers at 64°C.

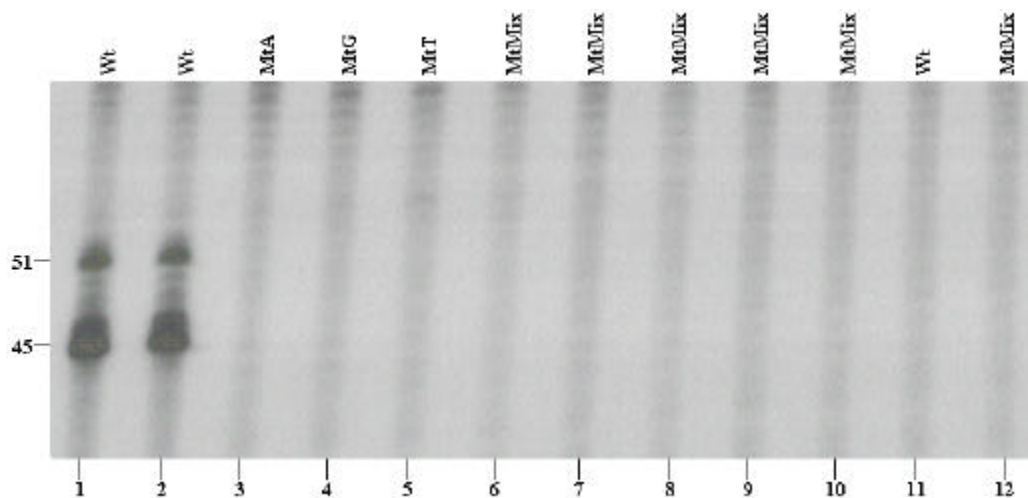


Figure 14. Autoradiograph of a second version LCR testing the Wt and Mt primers and oligonucleotide standards. Primers used are listed at the top of each lane. The template used in each lane is as follows: Lane 1 – HG. Lane 2 – HG. Lane 3 – HG. Lane 4 – HG. Lane 5 – HG. Lane 6 – ALstd (1pm). Lane 7 – GLstd (1pm). Lane 8 – TLstd (1pm). Lane 9 – Standard Mix (1pm). Lane 10 – HG. Lane 11 – Blank. Lane 12 – Blank.

The mutant primers were also tested for their ability in this LCR at 64°C. Mutant standards for the C1620A (MtA) mutation and the C1620G (MtG) mutation and the C1620T (MtT) mutation were tested separately and together as a mix along with the mutant primers for each of the mutation types (MtA, MtG, and MtT each separately with their corresponding mutations and as a mix). The only standard and mutant primer pair to ligate successfully at this temperature was the mutant T antisense primer with the mutant T standards (57bp). The MtT oligonucleotide standard was able to serve as template both by itself and in the mix.

The LCR mutant primers' ability to ligate with human mutant DNA was also tested in this LCR run. The MtG primer, both by itself and in a mutant primer mix was able to ligate human mutant C1620G DNA to give both sense (49bp) and antisense (55bp) products. The MtA primer, both by itself and in a mutant primer mix was also able to ligate human mutant C1620A DNA to give both sense (47bp) and antisense (53bp) products. The mutant DNA used in this run was human mutant DNA that was subjected to the first round of PCR with primer set S-MspIR then digested with *MspI*. The first PCR (primer set S-MspIR) used 200ng of wild-type human genomic DNA. The DNA was then subjected to a nested second round of PCR with primer set T-ZR2 and again digested with *MspI*. The mutant mix primers also showed some ability to ligate wild-type DNA. The wild-type and mutant primers did not form any product when run without any DNA in the reaction, evidence that the primers themselves can not form spontaneous products at this temperature.

Figure 17 was an attempt to refine the mutant standard for the C1620T mutation at 64°C. This mutation does not occur naturally, however, because it showed promise of being a good standard, the technique was altered in order to get both sense and antisense

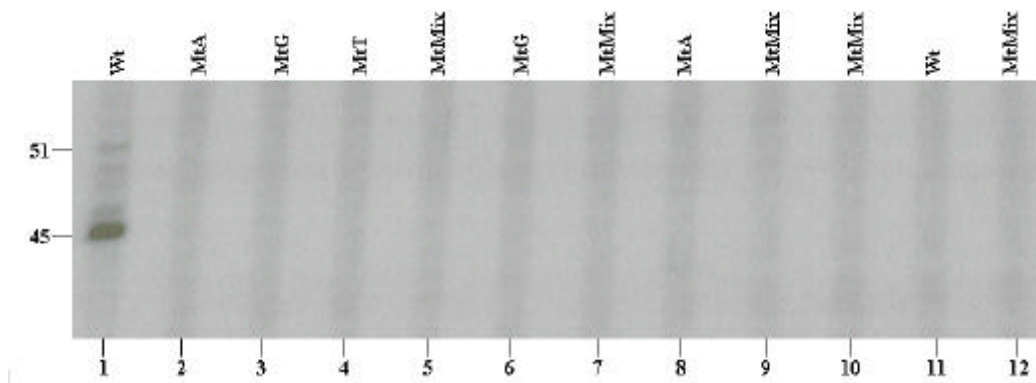


Figure 15. Autoradiograph of an LCR test with decreased concentration of oligonucleotide standards and mutant DNA with the Mt primers. Primers used are listed at the top of each lane. The template used in each lane is as follows: Lane 1 – HG. Lane 2 – ALstd (0.25pm). Lane 3 – GLstd (0.25pm). Lane 4 – TLstd (0.25pm). Lane 5 – Std Mix (0.25pm). Lane 6 – Mutant C1620G. Lane 7 – Mutant C1620G. Lane 8 – Mutant C1620A. Lane 9 – Mutant C1620A. Lane 10 – HG. Lane 11 – Blank. Lane 12 – Blank.

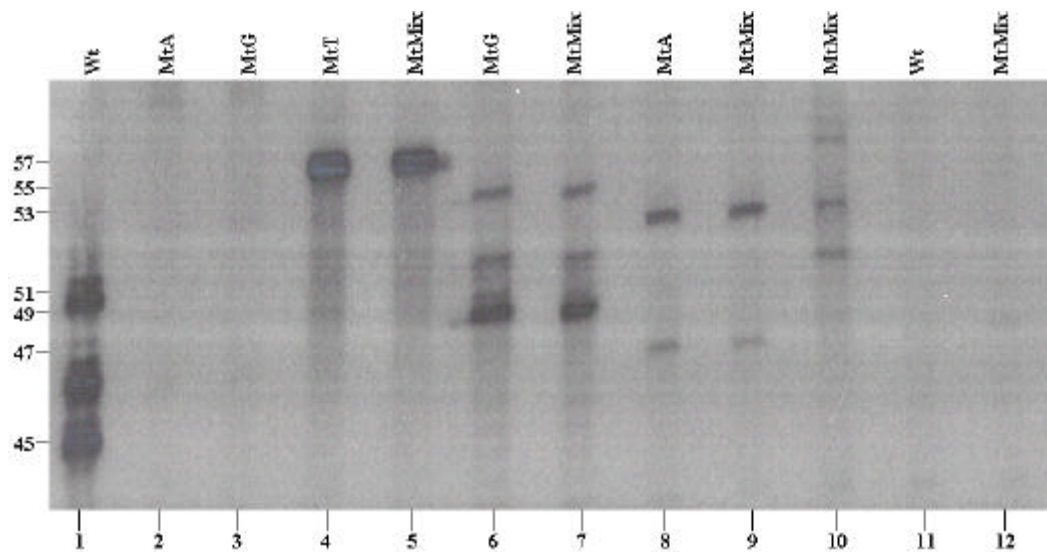


Figure 16. Autoradiograph of an LCR run at 64°C using HG DNA and mutant DNA with the wild-type and mutant primer sets. Primers used are listed at the top of each lane. The template used in each lane is as follows: Lane 1 – HG. Lane 2 – ALstd (1pm). Lane 3 – GLstd (1pm). Lane 4 – TLstd (1pm). Lane 5 – HG. Lane 6 – C1620G. Lane 7 – C1620G. Lane 8 – C1620A. Lane 9 – C1620A. Lane 10 – HG. Lane 11 – Blank. Lane 12 – Blank.

product formed. The human wild-type and mutant (C1620A) DNA was also cleaned with the Qiagen PCR clean-up kit in order to clean the extra bands seen between the wild-type sense and antisense bands. These results show that cleaning the PCR/RE product before running the LCR reaction did in fact remove the extra bands. The mutant C1620A LCR product did not show any difference between 'clean' and 'dirty' PCR/RE product.

The MtT oligonucleotide standards in this run were also diluted from 1 picomole per reaction down to 0.008 picomoles per reaction. It was believed that the large concentration of oligonucleotide standards compared to primers was interfering in the LCR reactions ability to form the sense strand product. Results showed that no amount of dilution could aid in producing the sense strand. If the other mutant primers behaved this way it would be very detrimental because it is the sense product of the LCR reaction that gives the actual base change that leads to hypochondroplasia. Having only the antisense product is adequate for evidence of mutation, however, in order to declare mutation with absolute certainty, both the sense and antisense bands must be present.

In order to increase the efficiency of the LCR reaction, the temperature was again lowered to 62°C. The MtT standard was also diluted from 0.016 picomoles down to 0.0001 picomoles per reaction. The 'cleaned' PCR product was used for wild-type and mutant C1620A template. The human mutant C1620G DNA was also tested at this new temperature. The DNA templates were products from the second digestion reaction after the second PCR (T-ZR2). 200ng of both wild-type human genomic and human mutant DNA were used in the first PCR.

The results of this new technique are shown in Figure 18. At the new temperature the 'clean' wild-type PCR product produced extra bands between the sense and antisense

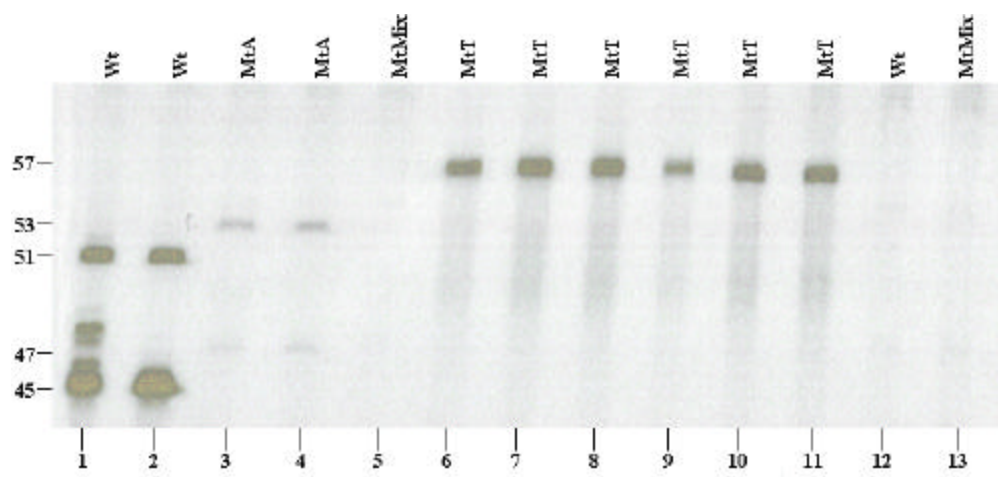


Figure 17. Autoradiograph of an LCR testing progressively decreasing concentrations of oligonucleotide standard T with the MtT primer. 'Clean' DNA was also tested in this run to compare the product bands with 'dirty' DNA. Primers used are listed at the top of each lane. The template used in each lane is as follows: Lane 1 – 'Dirty' HG. Lane 2 – 'Clean' HG. Lane 3 – 'Dirty' C1620A. Lane 4 – 'Clean' C1620A. Lane 5 – HG. Lane 6 – TLstd (1pm). Lane 7 – TLstd (0.5pm). Lane 8 – TLstd (0.25pm). Lane 9 – TLstd (0.125pm). Lane 10 – TLstd (0.0625pm). Lane 11 – TLstd (0.032pm). Lane 12 – Blank. Lane 13 – Blank.

bands. The MtT standards began to produce both sense and antisense bands with the oligonucleotide mutant standard at 0.016 picomoles in the reaction at this temperature.

With the LCR reaction at 62°C, many components of the assay were working with some degree of success. The human wild-type DNA was working as a template for the wild-type primers and the human wild-type DNA was not serving as template for any of the mutant primers. The wild-type and mutant primers were also not spontaneously forming LCR product in the absence of DNA. In addition, the mutant primers were forming both sense and antisense bands with the mutant primers at 62°C. The MtT standard was also serving as template for the MtT primers to form both sense and antisense bands at a concentration of 0.016 picomoles per reaction. Because all of these components were working with some degree of accuracy, a full selection process was attempted to achieve a 1-in-a-million detection sensitivity.

The results of the PCR/RE/LCR selection process are shown in Figure 19. The positive result with wild-type primers and wild-type DNA template ensured the LCR reaction was working successfully. The MtT oligonucleotide standard at a concentration of 0.002 picomoles also produced sense and antisense bands. The human mutant DNA was combined with human wild-type DNA at various concentrations to get varying degrees of sensitivity. The sensitivity of detection corresponds to the number of mutant genomes detected in the presence of 2×10^6 wild-type genomes (10^6 cells). For instance, 1 in 100 would correspond to 1 mutant genome in 100 wild-type cells. Table 14 gives the amounts of DNA used and the resulting sensitivities.

The LCR assay in Figure 19 showed bands produced with 6 µg of wild-type DNA with a mutant primer mix. The bands corresponded with the sense and antisense strands of

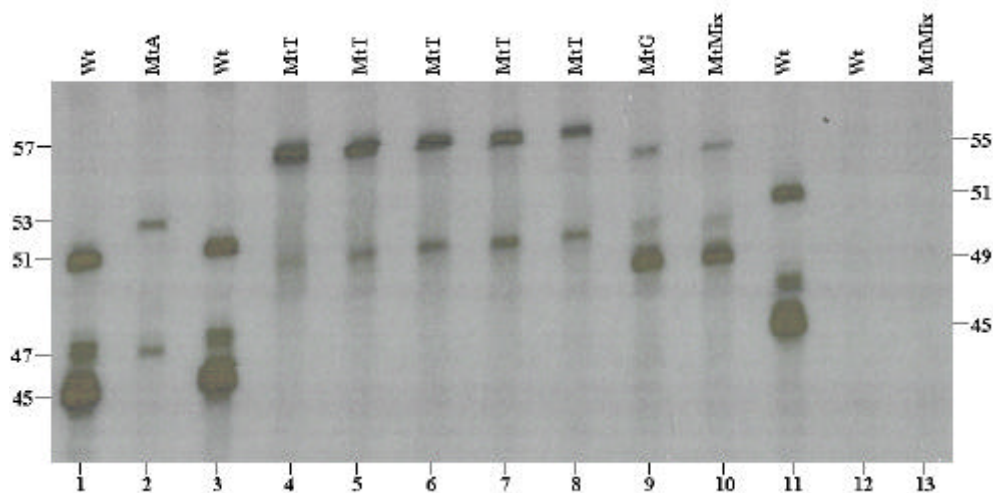


Figure 18. Autoradiograph of an LCR run at 62°C. This run was used to test progressive dilutions of the oligonucleotide mutant T standard. Note that the PAGE ran skewed and the size of the bands do not line up precisely from left to right. The scale on the left should be used for Lanes 1-8 and the scale on the right should be used for Lanes 9-13. Primers used are listed at the top of each lane. The template used in each lane is as follows: Lane 1 – ‘Clean’ HG. Lane 2 – ‘Clean’ C1620A. Lane 3 – ‘Clean’ C1620A. Lane 4 – TLstd (0.016pm). Lane 5 – TLstd (0.008pm). Lane 6 – TLstd (0.004pm). Lane 7 – TLstd (0.002pm). Lane 8 – TLstd (0.001pm). Lane 9 – C1620G. Lane 10 – C1620G. Lane 11 – C1620G. Lane 12 – Blank. Lane 13 – Blank.

the MtT primer set. This set had previously not appeared with other LCR runs. However, this was the first run using such a large amount of DNA, 6 µg compared with 200 ng. This run did show successful ligation of both sense and antisense wild-type primers with 6 µg of human wild-type DNA.

Table 14. Amount of mutant DNA combined with 6 µg of wild-type DNA to reach the desired sensitivities.

Wild-type DNA	Mutant DNA	Sensitivity
6 µg	600 ng	1 in 100
6 µg	0.6 ng	1 in 10,000
6 µg	0.06 ng	1 in 100,000
6 µg	0.006 ng	1 in 1,000,000

This assay was able to obtain sensitivity (ligation of both sense and antisense primers) of 1 in a 100 with the C1620G mutation. However, there was ligation of the MtT primers at each of the sensitivities. It is uncertain if these false positives came from spontaneous ligation, ligation from wild-type template, or ligation from mutant template.

This assay was also able to obtain sensitivities of 1 in 100 (sense and antisense band), 1 in 10,000 (antisense band), 1 in 100,000 (antisense band), and possibly 1 in 1,000,000 (very faint antisense band) with the C1620A mutation. However, there was also ligation of the MtT primers at each of the sensitivities as well.

9.5 Design of the Third Version of the LCR Assay at Site 1620

Because the second version of the LCR assay at site 1620 was not successful, a third version was designed. The principle behind changing the design was to try and decrease the number of false positives created with the MtT primers and do adapt the LCR primers for efficient ligation at 65°C rather than 62°C. This was attempted by shortening the L invariant primer and incorporating base changes in the MtT and MtA sense strand primers.

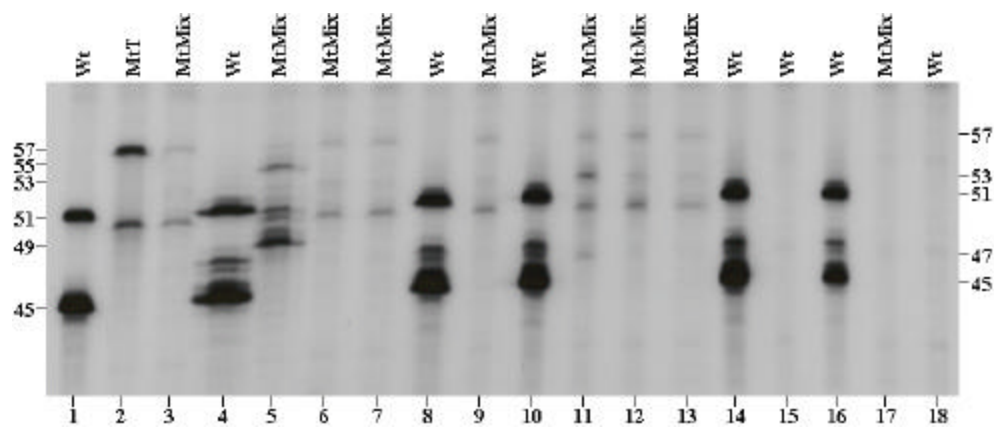


Figure 19. Autoradiograph of the 2nd version LCR with the selection process. Primers used are listed at the top of each lane. The template used in each lane is as follows: Lane 1 – HG. Lane 2 – TLstd (0.002pm). Lane 3 – 6ig Wt (with selection). Lane 4 – 6ig Wt (with selection). Lane 5 – C1620G (10^{-2}). Lane 6 – C1620G (10^{-4}). Lane 7 – C1620G (10^{-6}). Lane 8 – C1620G (10^{-6}). Lane 9 – 6ig Wt (with selection). Lane 10 – 6ig Wt (with selection). Lane 11 – C1620A (10^{-2}). Lane 12 – C1620A (10^{-4}). Lane 13 – C1620A (10^{-6}). Lane 14 – C1620A (10^{-6}). Lane 15 – Blank. Lane 16 – Blank. Lane 17 – Blank. Lane 18 – Blank.

Table 15 gives the new primers for the third version of the LCR assay. It should be noted that the Mts3GL and WtFGFR3c540s3L were not changed. The antisense discriminating primers were not altered either.

Table 15. LCR Version 3 primers and size in base pairs. The bolded bases denote a designed base pair change to coincide with the incorporated base pair changes from the PCR/RE series. The underscored bases in the variant primers indicate the base which must be present at base pair 1620 for ligation to be successful and yield product. The lower case bases are the base changes specific for the version 3 LCR.

LCR Primer	Size (bp)	Sequence (5' to 3')
Discriminating Set		
Sense Strand		
Mts3TL2	30	AAATAAAGGAAACACAACaAACATCATCAAT <u>I</u>
Mts3GL	28	ATAAAAGAAACACAAAAACATCATCAAG <u>G</u>
Mts3AL2	26	AAAAAAAAACACAACaAACATCATCAAA <u>A</u>
WtFGFR3c540s3L	24	AGGAAACACAAAAACATCATCAAC <u>C</u>
Antisense Strand		
WtFGFR3c540s3LR2	18	AAACAGGAGCCCAGCCG <u>G</u>
Mts3ALR2	20	AAAAACAGGAGCCCAGCCG <u>T</u>
Mts3GLR2	22	AAAAAAAAAAGGAGCCCAGCCG <u>C</u>
Mts3TLR2	24	AAAAAAAAAACAGGAGCCCAGCCG <u>G</u>
Invariant Set		
FGFR3c540s3L3	18	CGGCTGGGCTCCTGCACG
FGFR3c540s3LR3	33	TTGATGATGTTgTTGTGTTTCCCGATCATCTTC

Table 16. Sizes of LCR product, from both the sense and antisense strands, for the various wild type (Wt) and mutant (Mt) primers for the third LCR design.

DNA Strand	Wt	MtA	MtG	MtT
Sense	42	44	46	48
Antisense	51	53	55	57

Figure 20 gives the results of an LCR performed with a mixture of components from the second and third version of the LCR techniques. The purpose of this run was to determine which groups of invariant and discriminating primers worked the most efficiently together. Both L2 and L3 worked with LR3 to produce both sense and

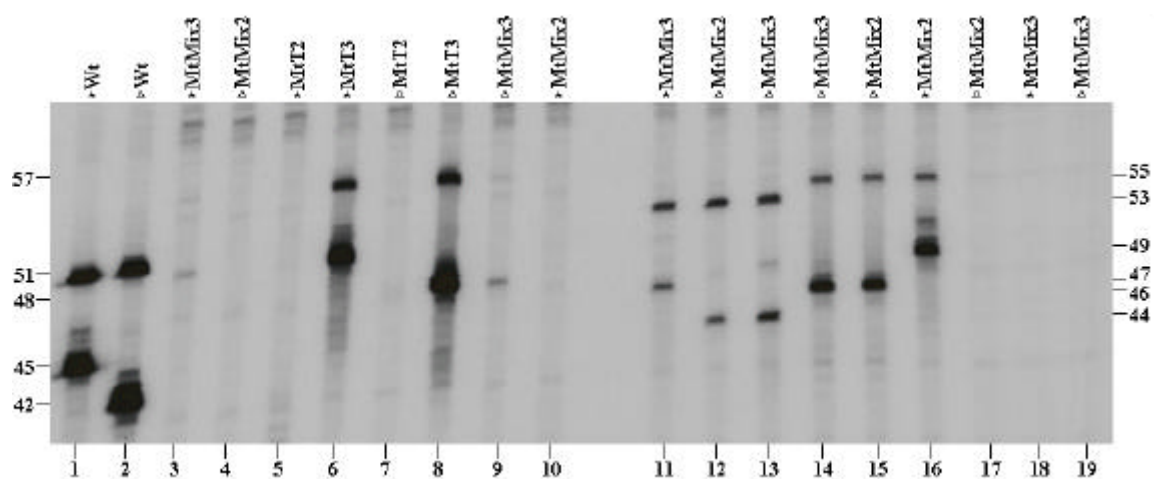


Figure 20. Autoradiograph of an LCR run at 65°C testing the compatibility of the 3rd version mutant primers with the 2nd and 3rd version invariant primers. Primers used are listed at the top of each lane. A '*' denotes version 2 invariant primers, a '□' denotes version 3 invariant primers. The template used in each lane is as follows: Lanes 1-10 – HG. Lanes 11-13 – C1620A. Lanes 14-16 – C1620G. Lanes 17-19 – Blank.

antisense bands (L2 and LR3: 51bp and 45bp; L3 and LR3: 51bp and 45bp). The invariant primer combinations L2/LR3 and L3/LR3 both failed to ligate with both versions 2 and version 3 mutant primer mixes using wild-type DNA as the template, indicating that neither combination should give a mutant false positive with wild-type DNA. However, both showed faint bands corresponding to ligation of the MtT primers.

The version 3 mutant primers for the 'T' mutation did, however, ligate to produce intense bands with wild-type template when the MtT primers were used alone with the L2/LR3 combination of invariant primers and the L3/LR3 combination. The version 2 MtT primer by itself did not produce bands at all when it was used with the L2/LR3 combination of invariant primers and the L3/LR3 combination, though.

The ability of the version 3 mutant primers and invariant primer combinations to ligate using human mutant C1620A and C1620G DNA as template was also tested in this run. The version 3 primers were able to form product with both C1620A and C1620G templates using both the L2/LR3 and L3/LR3 combinations. The version 2 primers also showed the ability to form product with both C1620A and C1620G templates using both the L2/LR3 and L3/LR3 combinations. These results also showed that the version 3 mutant primers would not spontaneously form ligation product with either the L2/LR3 or L3/LR3 invariant primers without the presence of DNA.

The results of the previous LCR run gave very mixed results, but it was determined that the third version LCR mutant primers and the L3/LR3 invariant primers would potentially give the best results. Figure 21 gives the results of the selection procedure with these new components. The LCR reaction was run at 62°C.

This run showed basically the same problems as the last run of the version 2 LCR reaction (Figure 19). While selection was reached at a sensitivity of 1 in 100 for the

C1620G mutation the C1620A sensitivity only reach 1 in 100, where previously it had possibly reached a little higher sensitivity. There was also a great deal of false positives with the formation of MtT LCR product whenever the MtT primers were present.

It was believed that the possible reason for low efficiency at lower sensitivities was that the MtT primers were interfering with the reaction. The LCR of the selection was then run without the presence of the MtT primers in the hope that a greater sensitivity could be obtained. Figure 22 gives the results from this run. Neither the C1620G nor the C1620A mutation reached a greater sensitivity than 1 in 100.

Because of the lack of progress at site 1620 for the hypochondroplasia mutation to this point, it was determined that the PCR/RE/LCR assay would not work. The results given here represent the most significant changes in the techniques of the assay. Many other variables were attempted to be altered, i.e. changing buffer pHs and concentrations, changing concentrations of various enzymes, changing lengths of restrictions, etc. However, no significant results were obtained by these attempts. Therefore, the attempt to develop an assay to determine the frequency of the C1620G/A hypochondroplasia causing mutation was terminated.

9.6 Allele Specific PCR Results for Site 1138

Many attempts were made previously in this lab to refine the PCR/RE/LCR technique for the G1138A/C achondroplasia mutation (personal communication, V.L. Wilson). As with the hypochondroplasia site, 1 in 1,000,000 sensitivity was never obtained. The PCR/RE/LCR technique discussed in Chapter 8 was the last version used by the lab and this technique was the basis for the next attempt to achieve sensitivity at site 1138.

Because the Needle-in-a-Haystack technique for determining frequency of mutation in a population of cells would not work, another approach was implemented. Since achondroplasia is more prevalent than hypochondroplasia in the population it was determined that an allele-specific PCR technique in conjunction with the selection process would be designed for the G1138A/C achondroplasia causing mutation.

This technique would use the same selection process as mentioned before in Chapter 8 to amplify progressively smaller amounts of the G1138A/C mutation in a large amount of wild-type DNA. At the point where the LCR was to determine the sensitivity, allele specific PCR was substituted.

The approach for the allele specific PCR was quite simple. The 3' end of three different oligonucleotide primers were designed to match with whatever base was present at site 1138. Table 17 gives the allele specific primers used in this technique. Figure 23 gives a schematic behind the design of the allele specific primers. The upstream primer in this technique was the allele specific primers while the downstream primer was primer YR2 (see table 6 for sequence).

Table 17. Primer sequences and sizes for the allele specific PCR technique at site 1138. The underscored bases correspond to site 1138.

Primer	Sequence (5'-3')	Size (bp)
asWtGG1138	GCATCCTCAGCCAC <u>G</u>	15
asMtAG1138	GCATCCTCAGCCACA <u>A</u>	15
asMtCG1138	GCATCCTCAGCCACC <u>C</u>	15

Figure 24 gives the initial trial run of the allele specific primers. This PCR was run at a temperature of 60°C. The asWt (allele specific wild-type) primer successfully primed and formed the correct 58bp product. However, both of the mutant primers also primed the wild-type DNA to form false positives. All of the allele specific primers failed to form

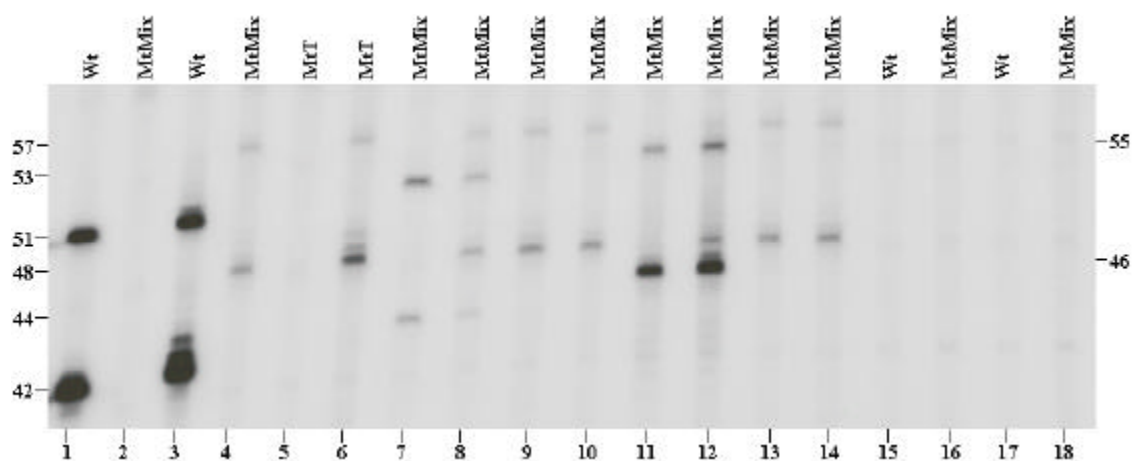


Figure 21. Autoradiograph of an LCR of the selection process to test acquired sensitivity. Primers used are listed at the top of each lane. The template used in each lane is as follows: Lane 1 – HG. Lane 2 – HG. Lane 3 – 6ig Wt (with selection). Lane 4 – 6ig Wt (with selection). Lane 5 – HG. Lane 6 – 6ig Wt (with selection). Lane 7 – C1620A. Lane 8 – C1620A (10^{-2}). Lane 9 – C1620A (10^{-4}). Lane 10 – C1620A (10^{-6}). Lane 11 – C1620G. Lane 12 – C1620G (10^{-2}). Lane 13 – C1620G (10^{-4}). Lane 14 – C1620G (10^{-6}). Lane 15 – Blank. Lane 16 – Blank. Lane 17 – Blank. Lane 18 – Blank.

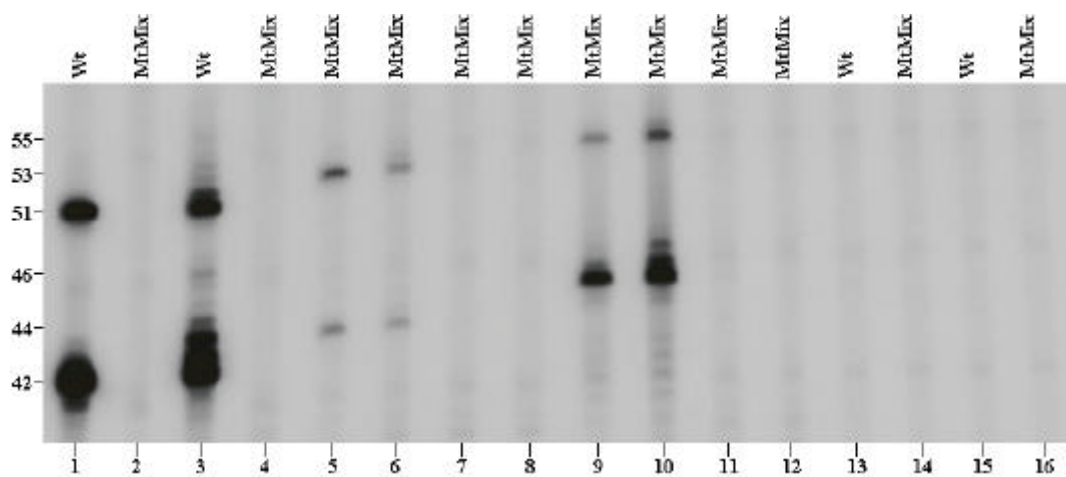


Figure 22. Autoradiograph of LCR selection process using a mutant primer mix that does not contain the MtT primers. Primers used are listed at the top of each lane. The template used in each lane is as follows: Lane 1 – HG. Lane 2 – HG. Lane 3 – 6 ig Wt (with selection). Lane 4 – 6 ig Wt (with selection). Lane 5 – C1620A. Lane 6 – C1620A (10^{-2}). Lane 7 – C1620A (10^{-4}). Lane 8 – C1620A (10^{-6}). Lane 9 – C1620G. Lane 10 – C1620G (10^{-2}). Lane 11 – C1620G (10^{-4}). Lane 12 – C1620G (10^{-6}). Lane 13 – Blank. Lane 14 – Blank. Lane 15 – Blank. Lane 16 – Blank.

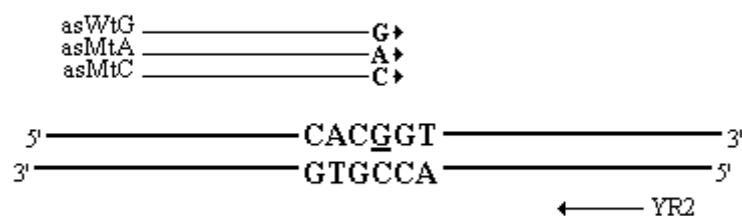


Figure 23. Schematic representation of the allele specific PCR at site 1138. The underscored 'G' represents site 1138. The asMtA primer will only prime if a 'A' is located at site 1138. The asMtC will only prime if there is a C at site 1138.

false positives in the reaction without DNA. The asMtA (allele specific mutant A) primer was also able to prime mutant G1138A template to form product, however, the asWt primer also primed to form product. The formation of product with asWt primers and G1138A mutant DNA template was an acceptable result because the achondroplasia mutation is heterozygous, therefore half of its genome is wild-type. However, the asMtC (allele specific mutant C) also formed product with the mutant G1138A template, suggesting that at 60°C there is not enough discrimination among the primers to prevent false positives.

The temperature of the PCR was then adjusted in order to refine the procedure and eliminate the false positives. The same assay was then run at 65°C, 58°C, and 59°C. The results at each of these temperatures are given in Figures 25-27. The new temperatures all gave the same false positives. The amount of template DNA was also cut in half in order to increase efficiency and decrease the template for possible false positives. Figure 28 gives these results which was the same as previous runs with the same amount of DNA.

It was determined that the allele specific primers did not have the ability to discriminate sufficiently at site 1138. The allele specific primers for both the wild type and the mutant G1138A mutation were then both redesigned. The base immediately upstream of the base corresponding to site 1138 was mismatched in order to help with the accuracy of the primers hydrogen bonding at site 1138. It was believed that with this mismatch, the base at site 1138 of the primer must match exactly with the base at site 1138 of the template in order to prime.

Figure 29 gives the results of the new primers at 65°C. The asWt primer produced product with wild-type DNA, however the asMtA2 primer also formed product with wild-

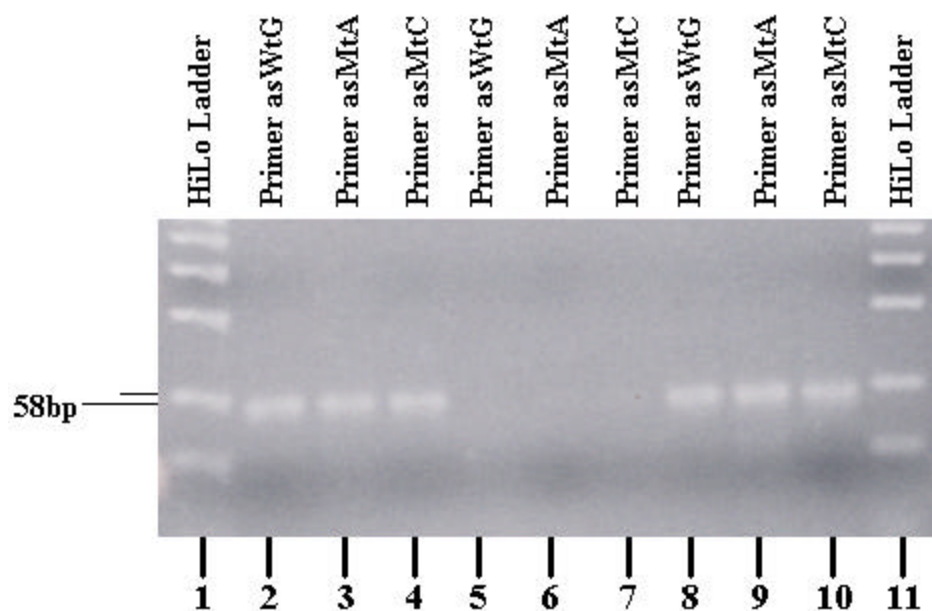


Figure 24. Agarose gel of the test run with the allele specific wild-type and mutant primers at 60°C. Lane 1 – HiLo Ladder. Lanes 2-4 – Wild-type DNA. Lanes 5-7 – Blank DNA. Lanes 8-10 – G1138A Mutant DNA. Lane 11 – HiLo Ladder.

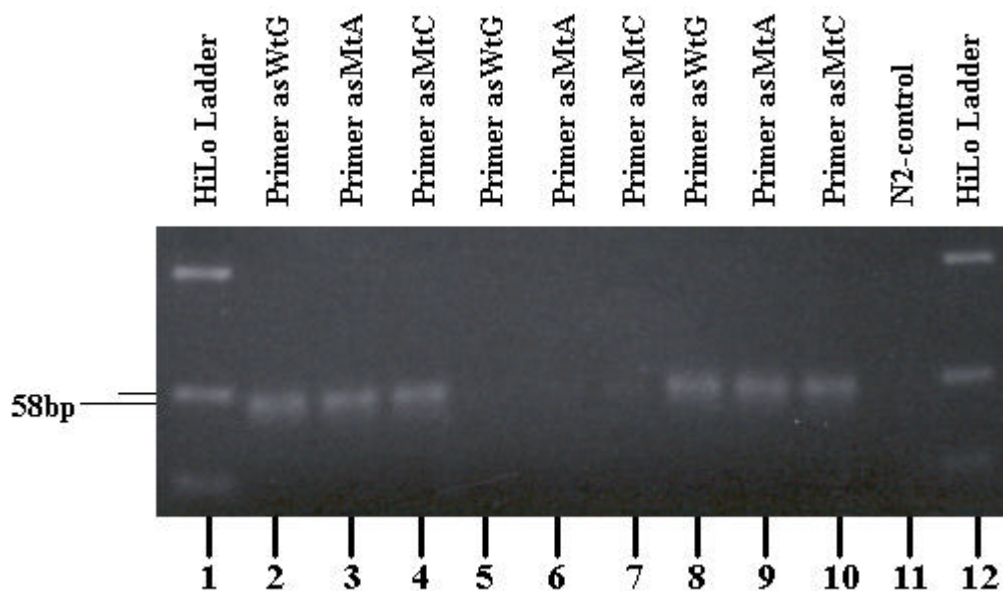


Figure 25. Agarose gel of the test run with the allele specific wild-type and mutant primers at 65°C. Lane 1 – HiLo Ladder. Lanes 2-4 – Wild-type DNA. Lanes 5-7 – Blank DNA. Lanes 8-10 – G1138A Mutant DNA. Lane 11 – Primer N2 used to test the PCR reaction mix, however, 65°C is not the optimal T_m . Lane 12 – HiLo Ladder.

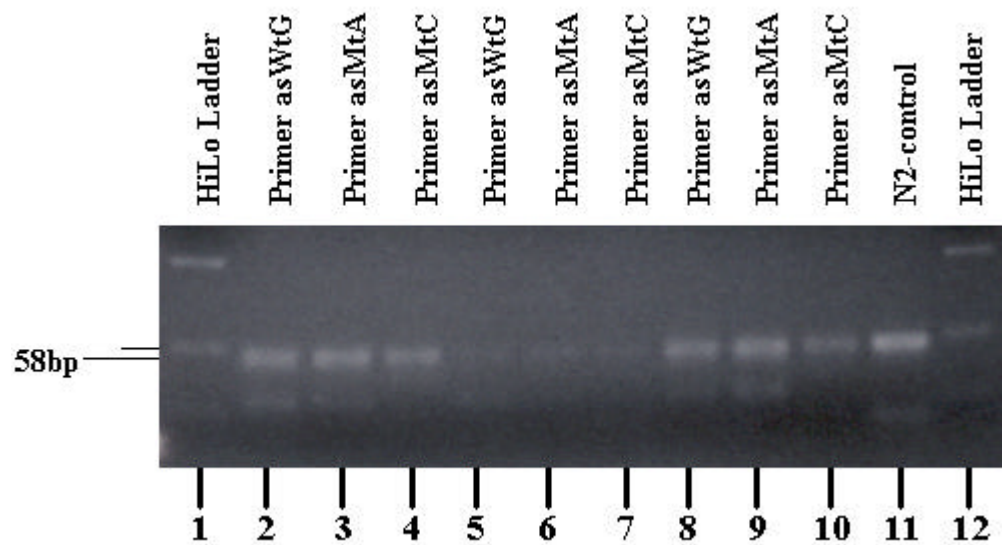


Figure 26. Agarose gel of the test run with the allele specific wild-type and mutant primers at 58°C. Lane 1 – HiLo Ladder. Lanes 2-4 – Wild-type DNA. Lanes 5-7 – Blank DNA. Lanes 8-10 – G1138A Mutant DNA. Lane 11 – Primer N2 used to test the PCR reaction mix. Lane 12 – HiLo Ladder.

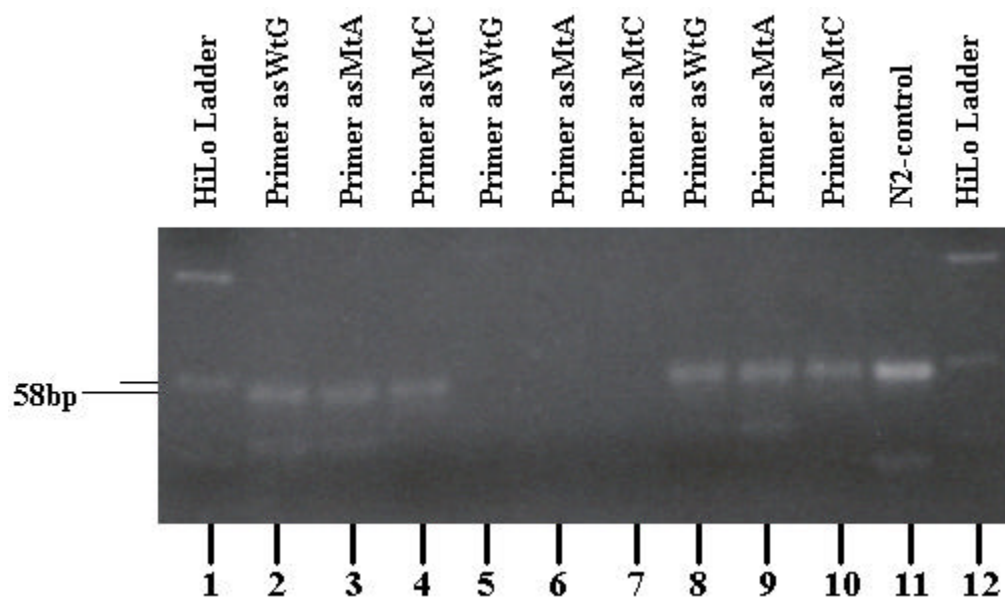


Figure 27. Agarose gel of the test run with the allele specific wild-type and mutant primers at 59°C. Lane 1 – HiLo Ladder. Lanes 2-4 – Wild-type DNA. Lanes 5-7 – Blank DNA. Lanes 8-10 – G1138A Mutant DNA. Lane 11 – Primer N2 used to test the PCR reaction mix. Lane 12 – HiLo Ladder.

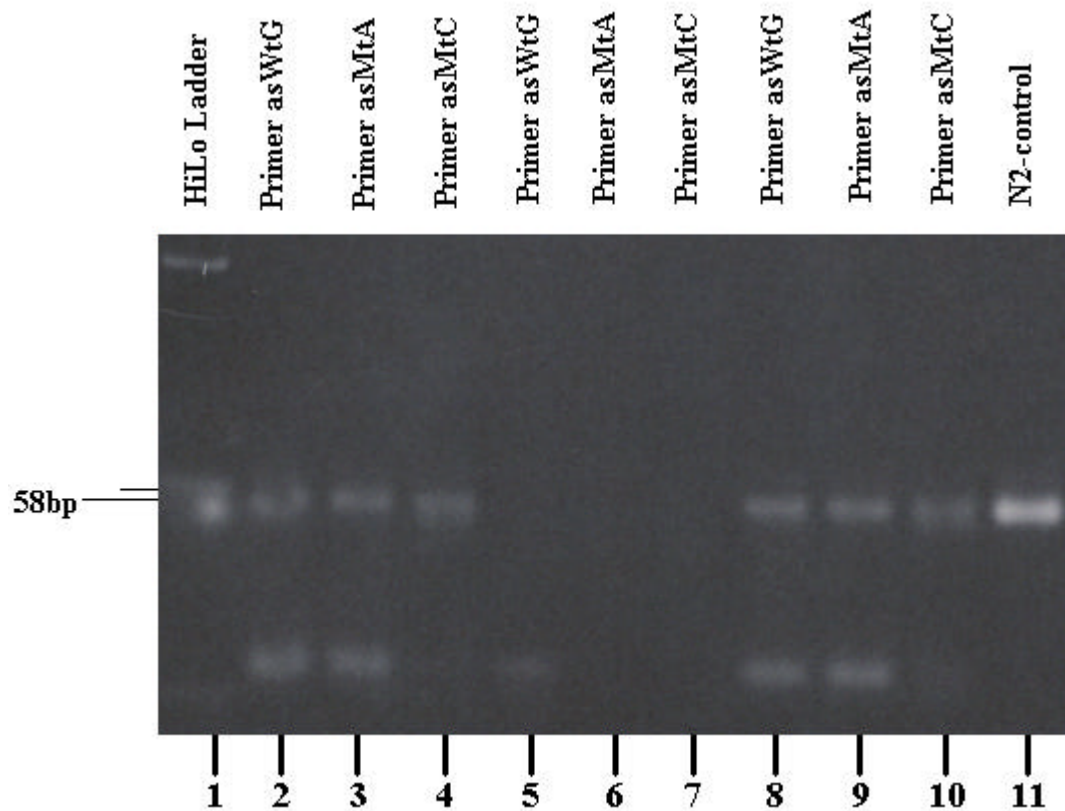


Figure 28. Agarose gel of the test run with the allele specific wild-type and mutant primers at 59°C using ½ the amount of template DNA. Lane 1 – HiLo Ladder. Lanes 2-4 – Wild-type DNA. Lanes 5-7 – Blank DNA. Lanes 8-10 – G1138A Mutant DNA. Lane 11 – Primer N2 used to test the PCR reaction mix.

Table 18. Primer sequences and sizes for the allele specific PCR technique at site 1138. The underscored bases correspond to site 1138. The bolded 'G' represents a mismatch incorporated to decrease the likelihood of false positives.

Primer	Sequence (5'-3')	Size (bp)
asWtG2G1138	CAGGCATCCTCAGCCAG <u>G</u>	18
asMtA2G1138	CAGGCATCCTCAGCCAG <u>A</u>	18

type DNA. The MtA2 primer did also make product with the G1138A mutant DNA template, however, it was not known if this was a false positive because of the results with the asMtA2 primer. The negative results of the various allele specific assays resulted in the termination of using allele specific PCR as a technique to determine the frequency of achondroplasia mutations in populations of sperm.

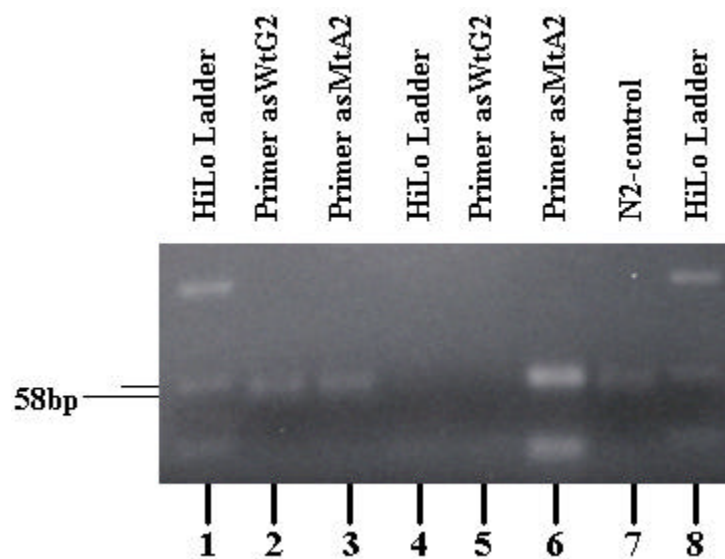


Figure 29. Agarose gel of the test run with second set of the allele specific wild-type and mutant primers. Lane 1 – HiLo Ladder. Lanes 2-3 – Wild-type DNA. Lanes 4-5 – Blank DNA. Lanes 6-7 – G1138A Mutant DNA. Lane 8 – HiLo Ladder.

CHAPTER 10. DISCUSSION

The development of a technique to measure the frequency of mutations in human gametes would prove very valuable to aid in understanding the processes that lead to inherited diseases. Two such inherited mutations that lead to disease are the G1138A/C and the C1620G/A FGFR-3 mutations. These two single base site mutations are the cause of achondroplasia and hypochondroplasia, respectively.

In an affected individual with either one of these diseases, the mutation occurs only on the paternal allele. In most situations, there is a *de novo* mutation because the father is not usually affected with the disease. Therefore, the mutation occurs spontaneously somewhere in the paternal germline prior to or during spermatogenesis. It is not known, however, if the mutation occurs from a single rogue sperm carrying the mutation or from a population of germ cells that are propagating the mutation. Knowing how many sperm cells carry one of the above mutations in the father of an affected individual would be very beneficial in understanding the occurrence and multiplication of germline mutations.

Previous research has demonstrated enormous sensitivity and specificity of the Needle-in-a-Haystack PCR/RE/LCR technique for single base mutations. This research has shown the technique to be capable of detecting not only a single base mutation in one cell in a large population of cells, but also the exact type of base mutation. By PCR amplification followed by restriction endonuclease digestion of wild-type DNA, mutations within a given area can be amplified while the amount of wild-type DNA can be reduced. The reliability of this mutant selection and detection process has been well documented (Wilson et al. 1999, 2000, 2001; Cerutti et al. 1994).

This project focused on developing an assay for measuring the frequency of achondroplasia and hypochondroplasia causing mutations in a large background of normal cells. PCR primers were developed to amplify the region around bases 1138 and 1620 of the FGFR-3 gene to amplify the G1138A/C and the C1620A/G mutations causing achondroplasia and hypochondroplasia, respectively. The 1138 PCR primers were designed to incorporate a *Bsa*II restriction site because a naturally occurring restriction enzyme did not exist which would digest the wild-type DNA and select for the mutant DNA.

Site 1620 provided many set backs from the beginning of the project. After numerous attempts to achieve sufficient digestion with the original restriction enzyme *Bsp*MI failed, new PCR primers were designed to incorporate the restriction enzyme *Msp*I. The incorporation of this new sequence for the digestion of wild-type DNA with *Msp*I was successful in obtaining sufficient digestion in order to proceed on to the LCR section of the assay.

The LCR technique for site 1620 showed limited success. The wild-type primers worked very well with both wild-type DNA and heterozygous mutant C1620A/G DNA. The mutant primers also worked very well with larger amounts of mutant template DNA. However, the mutant primers MtG and MtA were never able to successfully ligate with oligonucleotide standard templates for the mutations. The mutant primer MtT was, however, able to ligate with the oligonucleotide mutant T standard, but the C1620T mutation is not a proven naturally occurring mutation. The MtT primers also showed a zeal for product formation with almost any template at lower temperatures of the LCR reactions, thereby producing false positives.

Low sensitivities were obtained for both the C1620G and the C1620A mutations. These sensitivities, though, were only on the order of about 1 mutant cell in a population of 100 wild-type cells. This level of sensitivity is not adequate for the use of determining the frequency of these disease causing mutations in human sperm. This is because the mutations in the human population occur at a much lower level per live birth, something more on the level of achondroplasia which is about 1 in 15,000 to 1 in 40,000 live births.

The reasons behind failure of this approach to obtain adequate levels of sensitivity could be placed at many different levels. There may have been a problem with the actual selection process. Even though the PCR and RE reactions worked in the testing period, there is no way to prove the actual selection process worked. The difference between the amount of DNA used in each PCR and the number of PCR cycles the DNA was subjected to would be the two main reasons that the PCR/RE worked in the testing period and not in the selection process. For testing, 200 ng of DNA was subjected to about 120 total cycles of PCR amplification, while during the selection process, as little as 0.006 ng of DNA was subjected to only 65 cycles of PCR amplification. Also, the addition of increasing levels of primer and enzyme to the subsequent selection reactions might have caused interference with the final LCR, i.e. primer/dimer combinations, competitive inhibition, and mismatching. This is an unlikely scenario, though, because it was shown that pure DNA showed little more advantage for the LCR reaction than did DNA with reaction remnants.

More likely, the problems arose from limited specificity of the LCR primers themselves and the combinations in which they were used. The proper procedures were followed in the original design process to develop primers that would work well together and with the template DNA. However, predicting how well the reagents will actually work is sometimes a blind process. The only way to properly assure the right combinations is to

empirically test all of the primers against each other. However, this is a very time consuming and costly process. Slight modifications to the designed primers and the reaction properties are the only rational approaches to improving the techniques. All of these steps were followed, but to no avail.

The final consideration for failure of this technique is the region of the genome in which the work was focused. Through some, as yet unknown process, these sites on the FGFR-3 gene might be refractory or inaccessible to modern conventional molecular genetic techniques. These sites, once mutated, might form sequences which make it very hard for the enzymes used in the assay to work efficiently.

The mutation at site 1138 also provided many complications with previous work in the lab (Wilson et. Al, unpublished data). As with site 1620, the PCR/RE selection process was believed to be working properly, however, the LCR detection process never reached adequate levels of detection sensitivity. Because achondroplasia is such an important and prominent human genetic disease, new techniques were developed to try and reach the desired sensitivities at this site before attempting to reach the desired sensitivities at the hypochondroplasia mutation site 1620.

Allele specific PCR primers were then designed to detect the type of mutation at site 1138. This process would use the same PCR/RE selection process but use allele specific PCR for the detection process. These primers, however, primed nonspecifically to all template types, regardless of the mutations. Redesigned primers also failed to bind precisely to the correct template.

The reasons for failure at this site fall along the same lines as for the failure for site 1620. The selection process, the LCR primer combinations, and the region of the genome are all valid complications that might have occurred during the refinement of this

technique. The problems observed in the attempts for the molecular analysis of these FGFR-3 mutations may also represent clues as to why these single base mutations are prominent disease causing problems in the human population. The G1138A/C and the C1620G/A mutations might be naturally resistant to normal cellular repair and correction systems. This study might also argue the belief that the Needle-in-a-Haystack approach to studying low frequencies of mutated nucleotides in a large background of wild-type cells might not in fact be a universal technique.

CHAPTER 11. CONCLUSIONS

Future attempts at obtaining high sensitivities of detection of achondroplasia and hypochondroplasia causing mutations should not be deterred because of these failures. Progress has recently been achieved at site 1138 in the lab of Baker et al. (2000). They have recently reported that through their technique, they found the frequency of the achondroplasia causing mutation in the sperm of one sample (sperm of a man with an achondroplastic child) to be on the order of about 1 mutated sperm per 22,000 wild type sperm. Their method of determining the frequency was by using the Invader Operation System. However, this reported frequency is shaky at best due to the limitations of the Invader assay.

The Invader system is an isothermal, homogenous genotyping assay that uses fluorescence energy transfer as a detection method. The specificity of the Invader Operation System is believed to be able to discriminate mutant and wild-type alleles at a resolution of at least 1:1000. It should also be noted that the high end level of sensitivity of this assay is on the same level as the reported frequency of the mutation. Because there is not a very wide margin of error at this level of sensitivity, the validity of the mutation frequency occurring at 1 in 12,000 is difficult to believe with total certainty.

The interesting point behind this study, if it is indeed valid, is that the frequency of the mutation in this man's sperm falls along one of the low end estimates of the frequency of achondroplastic live births in the population, about 1 in 15,000. If this proves to be true, there may be no prenatal selection against the mutation, i.e. it does not come from a germline event from the father. It may in fact be a mutation in the sperm after maturation

that leads to disease. However, this does not explain the increased frequency of achondroplasia with increasing age of the father.

The ability to determine the frequency of paternal inherited diseases derived from germline mutations in a population of sperm is a very valuable tool. With such an assay, the frequency of the disease causing mutations could be determined in the germ cells of the father of an affected individual. Finally, the background of the mutation in the normal population could be determined. With all of these factors known about a given inherited disease, the picture clears and many theories can be applied from it to other sex specific inherited diseases. With this approach, environmental exposures and other exposures to toxic compounds could be evaluated for producing these mutations. It might also be determined that fathers of an affected child were previously exposed to a toxic mutagenic agent(s).

The study of germline mutations is a very important resource for discovering the reasons behind inherited mutations. The two diseases, achondroplasia and hypochondroplasia provide excellent models for determining sex specific germline mutation processes and how they impact second and third generations. Future endeavors should give more insight as to how to predict and alleviate the population of these important diseases.

REFERENCES

- Ago H, Kitagawa Y, Fujishima A, Matsuura Y, and Ichihashi M (1997). Crystal structure of basic fibroblast growth factor at 1.6 Å resolution. *Journal of Biochemistry* 110, 360-363.
- Alderborn A, Anvret M, Gustavson KH, Hagenas L, and Wadelius C (1996). Achondroplasia in Sweden caused by the G1138A mutation in FGFR3. *Acta Paediatr.* 85, 1506-1507.
- Andersen PE and Hauge M (1989). Congenital generalized bone dysplasias: a clinical, radiological, and epidemiological survey. *Journal of Medical Genetics* 26, 37-44.
- Baird A and Klagsbrun M (1991). Nomenclature meeting report and recommendations. *Annals of the New York Academy of Sciences* 638, xiii-xvi
- Baker MW, Lind D, Cox D, Wang L, Neri BP, and deArruda M. Detection of rare FGFR3 alleles in sperm samples using the Invader Operating System. American Society of Human Genetics Meeting.
- Basilico C and Moscatelli D (1992). The FGF family of growth factors and oncogenes. *Advances in Cancer Research* 59, 115-165.
- Beals RK (1969). Hypochondroplasia: a report of five kindreds. *Journal of Bone Joint Surgery* 51A, 728-736.
- Bellot F, Crumley G, Kaplow JM, Schlessinger J, Jaye M, and Dionne CA (1991). Ligand-induced transphosphorylation between different FGF receptors. *EMBO Journal* 10, 2849-2854.
- Bellus GA, Bamshad MJ, Przylepa K, Dorst J, Lee RR, Hurko O, Jabs EW, Curry CJR, Wilcox WR, Lachman RS, Rimoin DL, and Francomano CA (1999). Severe achondroplasia with developmental delay and acanthosis nigricans (SADDAN): Phenotypic analysis of a new skeletal dysplasia caused by the fibroblast growth factor receptor 3 Lys650Met mutation. *American Journal of Medical Genetics* 85, 53-65.
- Bellus GA, Gauden K, Zackai EH, Clark LA, Szabo J, Francomano CA, and Muenke M (1996). Identical mutations in three different fibroblast growth factor receptor genes in autosomal craniosynostosis syndromes. *Nature Genetics* 14, 174-176.
- Bellus GA, Hefferon TW, Ortiz de Luna RI, Hecht JT, Horton WA, Machado M, Kaitila I, McIntosh I, and Francomano CA (1995). Achondroplasia is defined by recurrent G380R mutation of FGFR3. *American Journal of Human Genetics* 56, 368-373.
- Bellus GA, Kelly DP, and Norris DA (2000). Activating mutations of fibroblast growth factor receptor 3 that cause acanthosis nigricans increase resistance to induce apoptosis in keratinocytes. *Journal of Investigative Dermatology* 114, 793(Abstract)

- Bellus GA, McIntosh I, Smith EA, Aylsworth AS, Kaitila I, Horton WA, Greenhaw GA, Hecht JT, and Francomano CA (1995). A recurrent mutation in the tyrosine kinase domain of fibroblast growth factor receptor 3 causes hypochondroplasia. *Nature Genetics* 10, 357-359.
- Bellus GA, Spector EB, Speiser PW, Weaver CW, Garber AT, Bryke CR, Israel J, Webster MK, Donoghue DJ, and Francomano CA (2000). Distinct missense mutations of the FGFR3 Lys650 codon modulate receptor kinase activation and the severity of the skeletal dysplasia phenotype. *American Journal of Human Genetics* 67, 1411-1421.
- Bird AP (1987). CpG-rich islands and the function of DNA methylation. *Nature* 321, 209-213.
- Bird AP (1980). DNA methylation and the frequency of CpG in animal DNA. *Nucleic Acid Research* 8, 1499-1504.
- Blanquet PR, Patte C, Fayein N, and Courtois Y (1989). Identification and isolation from bovine epithelial lens cells of two basic fibroblast growth factor receptors that possess bFGF-enhanced phosphorylation activities. *Biochemical and Biophysical Research Communications* 160, 1124-1131.
- Carlson KM (1994). Parent-of-origin effects in multiple endocrine neoplasia type 2A. *American Journal of Human Genetics* 55, 1076-1082.
- Cerutti P, Hussain C, Pourzand F, and Aguilar F (1994). Mutagenesis of the H-ras proto-oncogene and the p53 tumor suppressor gene. *Cancer Research* 54, 1934-1938.
- Colvin JS, Bohne BA, Harding GW, McEwen DG, and Ornitz DM (1996). Skeletal overgrowth and deafness in mice lacking fibroblast growth factor receptor 3. *Nature Genetics* 12, 390-397.
- Cooper DN and Youssoufian H (1997). The CpG dinucleotide and human genetic disease. *Human Genetics* 78, 151-155.
- Coughlin SR, Barr PJ, Cousens LS, Fretto LJ, and Williams LT (1988). Acidic and basic fibroblast growth factors stimulate tyrosine kinase activity *in vivo*. *Journal of Biological Chemistry* 263, 988-993.
- Crow JF (1997). The high spontaneous mutation rate: is it a health risk? *Proceedings of the National Academy of Science, USA* 94, 8380-8386.
- Crow JF (2000). The origins, patterns, and implications of human spontaneous mutation. *Nature Reviews Genetics* 1, 40-47.
- Deng C, Wynshaw-Boris A, Zhou F, Kuo A, and Leder P (1996). Fibroblast growth factor receptor 3 is a negative regulator of bone growth. *Cell* 84, 911-921.

- Deutz-Terlouw PP, Losekoot M, Aalfs CM, Hennekam RCM, and Bakker E (1998). Asn540Thr substitution in the fibroblast growth factor 3 tyrosine kinase domain causing hypochondroplasia. *Human Mutation* 1, 162-165.
- Deutz-Terlouw PP, Losekoot M, Aalfs CM, Hennekam RCM, and Bakker E (1998). Asn540Thr substitution in the fibroblast growth factor receptor 3 tyrosine kinase domain causing hypochondroplasia. *Human Mutation* 1, 162-165.
- Drake JW, Charlesworth Brian, Charlesworth D, and Crow JF (1998). Rates of spontaneous mutation. *Genetics* 148, 1667-1686.
- Driscoll D and Migeon BR (1990). Sex differences in methylation of single-copy genes in human meiotic germ cells: Implications for X chromosome inactivation, parental imprinting and origin of CpG mutations. *Somatic Cell Molecular Genetics* 16, 267-282.
- El-Maarri O, Olek A, Balaban B, Montag M, Van der Ven H, Urman B, Olek K, Caglayan SH, Walter J, and Oldeburg J (1998). Methylation levels at selected CpG sites in the factor VIII and FGFR3 genes, in mature female and male germ cells: implications for male driven evolution. *American Journal of Human Genetics* 63, 1001-1008.
- Fofanova OV, Takamura N, Kinoshita E, Meerson EM, Lijina VK, Nechvolodova OL, Evgrafov OV, Peterkova VA, and Yamashita S (1998). A missense mutation of C1659 in the fibroblast growth factor receptor 3 gene in Russian patients with hypochondroplasia. *Endocrinology Journal* 45, 791-795.
- Folkman J, Klagsbrun M, Sasse J, Wadzinski M, Ingber D, and Vlodavsky I (1988). A heparin-binding angiogenic protein - basic fibroblast growth factor - is stored within the basement membrane. *American Journal of Pathology* 130, 393-400.
- Francomano CA, Ortiz de Luna RI, Hefferon T, Bellus GA, Turner CE, Taylor E, Meyers DA, Blanton SH, Murray JC, McIntosh I, and Hecht JT (1994). Localization of the achondroplasia gene to the distal 2.5 Mb of human chromosome 4p. *Human Molecular Genetics* 3, 787-792.
- Glasser RL, Jiang W, Boyadjiev SA, Tran AK, Zachary AA, Van Maldergem L, Johnson D, Walsh S, Oldridge M, Wall SA, Wilkie AO, and Jabs EW (2000). Paternal origin of FGFR2 mutations in sporadic cases of Crouzon syndrome and Pfeiffer syndrome. *American Journal of Human Genetics* 66, 768-777.
- Gorlin RJ, Cohen MM, and Levin LS. *Syndromes of the Head and Neck*. 171-175. 90. New York, Oxford University Press.
- Grigeliuniene G, Hagenas L, Eklof O, Neumeyer L, Haereid PE, and Anvret M (1998). A novel missense mutation Ile538Val in the fibroblast growth factor receptor 3 in hypochondroplasia. *Human Mutation* 11, 333

- Haldane JBS (1947). The mutation rate of the gene for hemophilia and its segregation ratios in males and females. *Annals of Eugenics* 13, 262-271.
- Hassold T (1996). Human aneuploidy: Incidence, origin, and etiology. *Environmental Molecular Mutagenesis* 28, 167-175.
- Ikegawa S, Fukushima Y, Isomura M, Takada F, and Nakamura Y (1995). Mutations of the fibroblast growth factor receptor-3 gene in one familial and six sporadic cases of achondroplasia in Japanese patients. *Human Genetics* 96, 309-311.
- Johnson DE and Williams LT (1993). Structural and functional diversity in the FGF receptor multigene family. *Advances in Cancer Research* 60, 1-41.
- Jones KL. *Smith's Recognizable Patterns of Human Malformation*. 298. 88. Philadelphia, W.B. Saunders.
- Kan M, Wang F, Kan M, To B, Gabriel JL, and McKeehan WL (1996). Divalent cations and heparin/heparin sulfate cooperate to control assembly and activity of the fibroblast growth factor receptor complex. *Journal of Biological Chemistry* 271, 26143-26148.
- Kanai M, Goke M, Tsunekawa S, and Podolsky DK (1997). Signal transduction pathway of human fibroblast growth factor receptor 3. *The Journal of Biological Chemistry* 272, 6621-6628.
- Kato M, Wang H, Kainulainen V, Fitzgerald ML, Ledbetter S, Ornitz DM, and Bernfield M (1998). Physiological degradation converts the soluble syndecan-1 ectodomain from an inhibitor to a potent activator of FGF-2. *Nature Medicine* 4, 691-697.
- Keegan K, Johnson DE, Williams LT, and Hayman MJ (1991). Isolation of an additional member of the fibroblast growth factor receptor family. *Cell Biology* 88, 1095-1099.
- Kouhara H, Hadari YR, Spivak-Kroizman T, Schilling J, Bar-Sagi D, Lax I, and Schlessinger J (1997). A lipid-anchored Grb2-binding protein that links FGF-receptor activation of the Ras/MAPK signaling pathway. *Cell* 89, 693-702.
- Lee PL, Johnson DE, Cousens LS, Fried VA, and Williams LT (1989). Purification and complementary DNA cloning of a receptor for basic fibroblast growth factor. *Science* 57-60.
- LeMerrer M, Rousseau F, Legeai-Mallet L, Landais JC, Pelet A, Bonaventure J, Sanak M, Weissenbach J, Stoll C, and Munich A (1994). A gene for achondroplasia-hypochondroplasia maps to chromosome 4p. *Nature Genetics* 6, 318-321.
- Lemmon MA and Schlessinger J (1994). Regulation of signal transduction and signal diversity by receptor oligomerization. *Trends in Biochemical Science* 19, 459-463.

- Luo Y, Gabriel JL, Wnag F, Zhan X, Maciag T, Kan M, and McKeehan WL (1996). Molecular modeling and deletion mutagenesis implicate the nuclear translocation sequence in structural integrity of fibroblast growth factor-1. *Journal of Biological Chemistry* 271, 26876-26883.
- Maroteaux P and Lamy P (1964). Achondroplasia in man and animals. *Clinical Orthopedics* 33, 91-103.
- McKeehan WL, Adams PS, and Rosser MP (1984). Direct mitogenic effects of insulin epidermal growth factor, glucocorticoid cholera toxin, unknown pituitary factors and possibly prolactin but not androgen on normal rat prostate epithelial cells in serum-free primary cell culture. *Cancer Research* 44, 1988-2010.
- McKusick VA, Kelly TE, and Dorst JP (1973). Observations suggesting allelism of the achondroplasia and hypochondroplasia genes. *Journal of Medical Genetics* 10, 11-16.
- Meyers DK, Nicklas J, Munro IR, Pryzlepa KA, and Jabs EW (1995). Fibroblast growth factor receptor 3 (FGFR3) transmembrane mutation in Crouzon syndrome with acanthosis nigricans. *Nature Genetics* 11, 462-464.
- Miyamoto M, Naruo K-I, Seko C, Matsumoto S, Kondo T, and Kurokawa T (1993). Molecular cloning of a novel cytokine cDNA encoding the ninth member of the fibroblast growth factor family, which has a unique secretory property. *Molecular and Cellular Biology* 13, 4251-4259.
- Moloney DM, Slaney SF, Oldridge M, Wall SA, Sahlin P, Stenman G, and Wilkie AOM (1996). Exclusive paternal origin of new mutations in Apert syndrome. *Nature Genetics* 13, 48-53.
- Monsonneg-Orran E, Adar R, Feferman T, Segev O, and Yayon A (2000). The transmembrane mutation G380R in fibroblast growth factor receptor 3 uncouples ligand-mediated receptor activation from down-regulation. *Molecular Cell Biology* 20, 516-522.
- Mortier G, Nuytinck L, Craen M, Renard JP, Leory JG, and dePaepe A (2000). Clinical and radiographic features of a family with hypochondroplasia owing to a novel Asn540Ser mutation in the fibroblast growth factor receptor 3 gene. *Journal of Medical Genetics* 37, 220-224.
- Mortier G, Nuytinck L, Craen M, Renard JP, Leroy JG, and DePaepe A (2000). Clinical and radiographic features of a family with hypochondroplasia owing to a novel asn540ser mutation in the fibroblast growth factor receptor 3 gene. *Journal of Medical Genetics* 37, 220-224.
- Moscatelli D (1987). High and low affinity binding sites for basic fibroblast growth factor on cultured cells: absence of a role for low affinity binding in the stimulation of plasminogen activator production by bovine capillary endothelial cells. *Journal of Cellular Physiology* 131, 123-130.

- Moy FJ, Safran M, Seddon AP, Kitchen D, Bohlen P, Aviezer D, Yayon A, and Powers R (1997). Properly oriented heparin-decasaccharide-induced dimers are the biologically active form of basic fibroblast growth factor. *Biochemistry* 36, 4782-4791.
- Murdoch JL, Walker BA, Hall JG, Abbey H, Smithe KK, and McKusick VA (1970). Achondroplasia - genetic and statistical survey. *Annals of Human Genetics*, London 33, 227-244.
- Murgue B, Tsunekawa S, Rosenberg I, deBeaumont M, and Podolsky DK (1994). Identification of a novel variant form of fibroblast growth factor receptor 3 (FGFR3 IIIb) in human colonic epithelium. *Cancer Research* 54, 5206-5211.
- Oberklaid F, Danks DM, Jensen F, Stace L, and Rosshandler S (1979). Achondroplasia and hypochondroplasia: Comments on frequency, mutation rate and radiological features in skull and spine. *Journal of Medical Genetics* 16, 140-146.
- Oller AR, Broek WV, Conrad M, and Topal MD (1991). Ability of DNA and spermidine to affect the activity of restriction endonucleases from several bacterial species. *Biochemistry* 30, 2543-2549.
- Orioli IM, Castilla EE, Scarano G, and Mastroiacovo P (1995). Effect of paternal age in achondroplasia, thanatophoric dysplasia and osteogenesis imperfecta. *American Journal of Human Genetics* 59, 209-217.
- Perez-Castro AV, Wilson J, and Altherr MR (1997). Genomic organization of the human fibroblast growth factor receptor 3 (FGFR3) gene and comparative sequence analysis with the mouse Fgfr3 gene. *Genomics* 41, 10-16.
- Peters K, Ornitz D, Werner S, and Williams L (1993). Unique expression pattern of the FGF receptor 3 gene during mouse organogenesis. *American Journal of Human Genetics* 155, 423-430.
- Plotnikov AN, Schlessinger J, Hubbard SR, and Mohammadi M (1999). Structural basis for FGF receptor dimerization and activation. *Cell* 98, 641-650.
- Powers CJ, McLeskey SW, and Wellstein A (2000). Fibroblast growth factors, the receptors, and signaling. *Endocrine-Related Cancer* 7, 165-197.
- Prinos P, Costa T, Kilpatrick MW, and Tsipouras P (1995). A common FGFR3 gene mutation in hypochondroplasia. *Human Molecular Genetics* 4, 2097-2101.
- Raffioni S, Zhu YZ, Bradshaw RA, and Thompson LM (1998). Effect of transmembrane and kinase domain mutations on fibroblast growth factor 3 chimera signaling in PC12 cells. *Journal of Biological Chemistry* 273, 35250-35259.
- Ramaswami U, Rumsby G, Hindmarsh PC, and Brook CGD (1998). Genotype and phenotype in hypochondroplasia. *Journal of Pediatrics* 133, 99-102.

- Ravenna F (1913). Achondroplasie et chondrohypoplasie: contribution clinique. *N Iconogr Salpetriere* 26, 157-184.
- Risch N, Reich EW, Wishnick MM, and McCarthy JG (1987). Spontaneous mutation and parental age in humans. *American Journal of Human Genetics* 41, 218-248.
- Rosendaal FR, Brocker-Vriends A, Van Houweligen C, Smit C, Verekamp I, Van Dijk H, Suurmeijer TP, and et al (1990). Sex ratio of the mutation frequencies in hemophilia A: estimations and meta-analysis. *Human Genetics* 86, 139-146.
- Rousseau F, Bonaventure J, Legeai-Mallet L, Pelet A, Rozet JM, Maroteaux P, LeMerrer M, and Munnich A (1994). Mutations in the gene encoding fibroblast receptor growth factor receptor-3 in achondroplasia. *Nature* 371, 252-254.
- Rousseau F, Bonaventure J, Legeai-Mallet L, Schmidt H, Weissenbach J, Maroteaux P, Munnich A, and LeMerrer F (1996). Clinical and genetic heterogeneity of hypochondroplasia. *Journal of Medical Genetics* 33, 749-752.
- Rousseau F, El Ghouzzi V, Delezoide AL, Legeai-Mallet L, LeMerrer M, Munnich A, and Bonaventure J (1996). Missense FGFR3 mutations create cysteine residues in thanatophoric dwarfism type I (TDI). *Human Molecular Genetics* 5, 509-512.
- Rubin JS, Osada H, Finch PW, Taylor WG, Rudikoff S, and Aaronson SA (1989). Purification and characterization of a newly identified growth factor specific for epithelial cells. *PNAS* 86, 802-806.
- Schorderet DF and Gartler SM (1992). Analysis of CpG suppression in methylated and nonmethylated species. *Proceedings of the National Academy of Science, USA* 89, 957-961.
- Shiang R, Thompson LM, Zhu YZ, Church DM, Fielder TJ, Bocian M, Winokur ST, and Wasmuth JJ (1994). Mutations in the transmembrane domain of FGFR3 cause the most common genetic form of dwarfism, achondroplasia. *Cell* 78, 335-342.
- Sommer SS and Ketterling RP (1996). The factor IX gene as a model for analysis of human germline mutations: an update. *Human Molecular Genetics* 5, 1505-1514.
- Spivak-Kroizman T, Lemmon MA, Dikic I, Ladbury JE, Pinchasi D, Huang J, Jaye M, Crumley G, Schlessinger J, and Lax I (1994). Heparin-induced oligomerization of FGF molecules is responsible for FGF receptor dimerization activation and cell proliferation. *Cell* 79, 1015-1024.
- Stoilov I, Kilpatrick MW, Tsipouras P, and Costa T (1995). Possible genetic heterogeneity in hypochondroplasia. *Journal of Medical Genetics* 32, 492-493.
- Stoll C, Dott B, Roth MP, and Alembik Y (1989). Birth prevalence rates of skeletal dysplasias. *Clinical Genetics* 35, 88-92.

- Superti-Furga A, Eich G, Bucher HU, Wisser J, Giedion A, Gitezlmann R, and Steinmann B (1995). A glycine 375-to-cysteine substitution in the transmembrane domain of the fibroblast growth factor receptor-3 in a newborn with achondroplasia. *European Journal of Pediatrics* 154, 215-219.
- Tavormina PL, Bellus GA, Webster MK, Bamshad MJ, Fraley AE, McIntosh I, and Szabo J (1999). A novel skeletal dysplasia with developmental delay and acanthosis nigricans is caused by a Lys650Met mutation in the fibroblast growth factor receptor 3 (FGFR3) gene. *American Journal of Human Genetics* 64, 722-731.
- Tavormina PL, Shiang R, Thompson LM, Zhu YZ, WilkinDJ, LachmanRS, Wilcox WR, Rimoin DL, Cohn DM, and Wasmuth JJ (1995). Thanatophoric dysplasia (types I and II) caused by distinct mutations in fibroblast growth factor receptor 3. *Nature Genetics* 9, 321-328.
- Thompson LM, Plummer S, Schalling M, Altherr MR, Gusella JF, Housman DE, and Wasmuth JJ (1991). A gene encoding fibroblast growth factor receptor isolated from the Huntington disease gene region of human chromosome 4. *Genomics* 11, 1133-1142.
- Tsai FJ, Wu JY, Tsai CH, and Chang JG (1999). Identification of a common N540K mutation in 8/18 Taiwanese hypochondroplasia patients: further evidence for genetic heterogeneity. *Clinical Genetics* 55, 279-280.
- Vajo Z, Francomano CA, and Wilkin DJ (2000). The molecular and genetic basis of fibroblast growth factor receptor 3 disorders: The achondroplasia family of skeletal dysplasias, Muenke craniosynostosis, and Crouzon syndrome with acanthosis nigricans. *Endocrine Reviews* 21, 23-39.
- Velinov M, Slaugenhaupt SA, Stoilov I, Scott CI, Gusella JF, and Tsipouras P (1994). The gene for achondroplasia maps to the telomeric region of chromosome 4p. *Nature Genetics* 6, 314-317.
- Vogel F and Motulsky A *Human genetics: problems and approaches*, 3d ed. (Berlin: Springer-Verlag).
- Vogel F and Rathenberg R (1975). Spontaneous mutation in man. *Advances in Human Genetics* 5, 223-318.
- Walker BA, Murdoch JL, McKusick VA, Langer LO, and Beals RK (1971). Hypochondroplasia. *American Journal of Disabled Children* 122, 95-104.
- Wang JK, Xu H, Li HC, and Goldfarb M (1996). Broadly expressed SNT-like proteins link FGF receptor stimulation to activators of Ras. *Oncogene* 13, 721-729.
- Wilkin DJ, Szabo JK, Cameron R, Henderson S, Bellus GA, Mack ML, Kaitila I, Loughlin JL, Munnich A, Sykes B, Bonaventure J, and Francomano CA (1998). Fibroblast growth factor receptor 3 (FGFR3) mutations in sporadic cases of

achondroplasia occur exclusively on the paternally derived chromosome.
American Journal of Human Genetics 63, 711-716.

Winterpacht A, Hilbert K, Stelzer C, Schweikardt T, Decker H, Segerer A, and Spranger J (2000). A novel mutation in FGFR-3 disrupts a putative N-glycosylation site and results in hypochondroplasia. *Physiologic Genomics* 2, 9-12.

Zabel BU, Hilbert H, Beck M, Stelzer C, Wildhardt A, Winterpacht A, and Spranger J (2000). Achondroplasia phenotype due to novel FGFR3 mutation. *American Journal of Human Genetics* 67, 388(Abstract)

Zhang J, Cousens LS, Barr PJ, and Sprang SR (1991). Three-dimensional structure of human basic fibroblast growth factor, a structural homolog of interleukin 1 α . *PNAS* 88, 3446-3450.

VITA

Andrew T. Daters was born in 1975 in Memphis, Tennessee. He graduated high school in 1993 from Catholic High School for Boys in Little Rock, Arkansas. He then went on to receive a Bachelor of Science degree in biology from Washington and Lee University in 1997. While at Washington and Lee University, Andrew played on the varsity soccer team and lettered for four years. He was also a member of the Sigma Chi fraternity.

In the fall of 1999, Andrew started his master's program at Louisiana State University in the department of Veterinary Physiology, Pharmacology, and Toxicology. In the fall of 2000, he started in the Doctor of Veterinary Medicine program, also at Louisiana State University. The fall of 2000 was a very busy year for him not only because of the start of the DVM program, but also because he married the beautiful Anna Caller James. Andrew plans on finishing his veterinary schooling in 2004 and his doctoral program shortly thereafter.